Journal Pre-proof

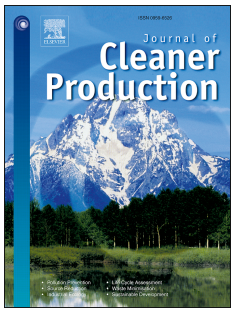

The state-of-the-art development of biochar based photocatalyst for removal of various organic pollutants in wastewater

Mahesan Naidu Subramaniam, Zhentao Wu, Pei Sean Goh, Shouyong Zhou

PII: S0959-6526(23)03645-4

DOI: https://doi.org/10.1016/j.jclepro.2023.139487

Reference: JCLP 139487

To appear in: *Journal of Cleaner Production*

Received Date: 6 July 2023

Revised Date: 14 October 2023

Accepted Date: 22 October 2023

Please cite this article as: Subramaniam MN, Wu Z, Goh PS, Zhou S, The state-of-the-art development of biochar based photocatalyst for removal of various organic pollutants in wastewater, *Journal of Cleaner Production* (2023), doi: https://doi.org/10.1016/j.jclepro.2023.139487.

The state-of-the-art development of biochar based photocatalyst for removal of various organic pollutants in wastewater

Mahesan Naidu Subramaniam[1], Zhentao Wu[1]*, Pei Sean Goh[2], Shouyong Zhou[3]

[1]Energy and Bioproduct Research Institute, Aston University, Aston St, Birmingham B4 7ET, United Kingdom

[2]Advanced Membrane Technology Research Center, University Teknologi Malaysia, 81300, Skudai, Johor, Malaysia

[3]Jiangsu Engineering Laboratory for Environmental Functional Materials, Jiangsu Key Laboratory for Biomass-based Energy and Enzyme Technology, School of Chemistry and Chemical Engineering, Huaiyin Normal University, No. 111 West Changjiang Road, Huaian 223300, Jiangsu Province, PR China

Corresponding email: z.wu7@aston.ac.uk

Abstract

The use of biochar (BC) as a substrate and dopant in developing composite biochar-based photocatalysts (BBP) has proven to be highly promising in advancing wastewater treatment technology. This review focuses on the development of BBP using agricultural and poultry waste-derived BC to mitigate organic pollutants in water, with emphasis on the synthesis technique employed for the preparation of various BBP. Various techniques for preparing BC and BBP, along with its features and physico-chemical properties, are discussed in detail. The review then delves into the role of BC in influencing the inherent properties of the BBP, particularly in reducing band gap, acting as an electron sink or reservoir, increasing surface active regions, and improving charge separation. Furthermore, the review outlines the synergistic improvement brought about by BC in BBP, specifically in terms of the photodegradation of different classes of pollutants, i.e. pharmaceutical waste, dye from the textile industry, and phenolic compounds. Lastly, the crucial challenges associated with the practical employment of BBP in real-time applications, such as scaling up, long-term stability, and retrofitting into existing wastewater remediation technologies are elaborated. This review will provide significant insights for readers evaluating the sources of BC used as substrates and the methods employed to develop efficient BBP for the remediation of various organic pollutants.

Keywords: biochar; photocatalyst; water treatment; organic pollutants

1.0 Introduction

Access to potable water safe for human consumption is becoming increasingly scarce for several reasons. These reasons include the rising rate of consumption, rapid industrialization and urbanization, and the depletion of clean water sources. According to reports published by the World Wildlife Foundation, approximately 1.1 billion people worldwide do not have consistent access to clean water, and nearly one-fourth of the global population experiences water scarcity at least once per month ("Water Scarcity | Threats | WWF," n.d.). The increasing use of fresh water also leads to the discharge of various types of wastewaters, another significant issue to be addressed. A recent study suggests that the current annual production of wastewater worldwide is estimated to be around 380 billion cubic meters (Qadir et al., 2020). Moreover, global wastewater generation is found to contain numerous persistent organic pollutants (POPs) which are harmful chemical substances that resist natural degradation and can enter different natural food chains through bioaccumulation. Improperly treated wastewater discharged into the environment can cause significant problems for various stakeholders. This is because such wastewater can have undesirable impacts on the ecosystem and pose a threat to public health (Wear et al., 2021).

One of the most actively researched techniques to address the harmful effects of POP-laden wastewater is photocatalysis. This process has shown significant promise as an environmentally friendly, sustainable, and straightforward method for eliminating various pollutants that may be present in different types of wastewaters. Nanomaterials, including titanium dioxide (TiO_2), iron (III) oxide (Fe_2O_3), zinc oxide (ZnO), ruthenium (IV) oxide (RuO), and silicone oxide (SiO_2), have been extensively employed as photocatalysts to break down different types of POPs, such as phenolic compounds, pharmaceutical compounds, dyes, and more (Elgohary et al., 2021). While the term POP is commonly used for organochlorine pesticides, such industrial chemicals, polychlorinated biphenyls (PCB) and unintentional by-products of many industrial processes, especially polychlorinated dibenzo-p-dioxins (PCDD) and dibenzofurans (PCDF), textile effluent can also be included in this category. Recent research articles have highlighted the presence of toxic dyes along with various heavy metals, such as mercury, chromium, cadmium, lead, and arsenic (Al-Tohamy et al., 2022). While other treatment technologies such as separation, flocculation and coagulation can effectively remove such pollutants, they produce waste by-products which would require secondary treatment for complete removal. On the other hand, photocatalysis aims to degrade those waste into harmless by-products. These catalysts are highly researched due to their chemical stability, low toxicity,

and sensitivity to ultraviolet (UV) light irradiation for activation. This sensitivity is due to the large band gaps of photocatalysts which only respond to UV light. While these catalysts have shown success in removing pollutants from wastewater, there are limitations that hinder their upscaling efforts. One significant limitation is that these photocatalysts require a dedicated UV light source for continuous photodegradation of pollutants. Additionally, poor recyclability also impacts their upscaling efforts. Researchers have explored different options to endow photocatalysts with visible light sensitivity, which offers many benefits such as visible light activation, reduced recombination rate, and reduced band gap for lower activation energy. While metal and non-metal options have been explored, the use of biochar (BC) as an eco-friendly dopant has emerged as one of the most promising techniques due to its inherent properties. BC has a large surface area, high porosity, high stability, is abundantly available, and low in cost. The availability of BC is due to the increasing demand for bio-waste from sectors such as agriculture, forestry, and food. The potential use of BC in wastewater treatment, agricultural fertilizers, pollutant removal from various environmental sources, and renewable energy adds significant value to the generation of BC from waste materials (Hama Aziz et al., 2023). In the current body of literature, there are several reviews that discusses the use of BC composite photocatalysts for the remediation of organic pollutants and micropollutants in the environment (Fito et al., 2022; Sutar et al., 2022). However, while previous reviews have focused on the formation of BC and a general overview of its application in waste remediation, this review will place greater emphasis on two specific aspects: the synthesis techniques for biochar based photocatalyst (BBP) and the role of BC in such composite BBP for the remediation of various organic pollutants.

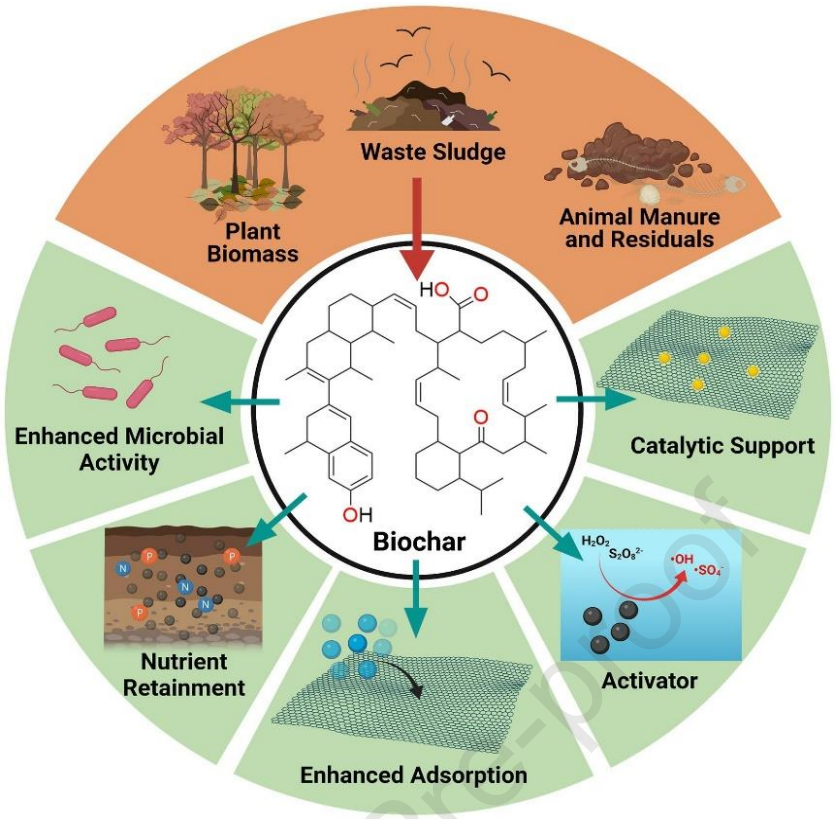

Figure 1 Overview of key BC feedstock sources and their applications (Yuan et al., 2022)

This review paper focuses on the use of BC in developing BC-based photocatalyst (BBP). The preparation techniques used to develop BC, as well as the catalytic improvement brought about when incorporated with traditional photocatalyst, are discussed in detail. The potential of BC as a substrate and dopant to improve the catalytic efficiency of different heterogeneous catalysts, and the efficiency of these catalysts in treating wastewaters laden with POPs, are explored. The mechanism involved in the removal of these pollutants, and the role BC plays in such mechanisms, are also examined. The review paper concludes by discussing the challenges faced and possible future endeavours that would be fruitful in furthering the case of BC as a viable material in the synthesis of BBP for the remediation of POPs. The scope of this review is limited to the use of BC for the remediation of pharmaceutical waste, dyes, and phenolics via photocatalysis. This scope was based on studying the presently available literature, where we believe that there is a need to place emphasis on remedying these forms of pollutants present in our waterways. While there are a couple of review papers discussing the use of BC in the development of photocatalysts, they primarily focus on the impact of different dopant classes in general. This review paper, on the other hand, provides a more in-depth examination of the synthesis techniques of BBP and how they affect the characteristics of the resulting BBP, as well as their inherent performance among different varieties of POPs. It is expected that this

review will provide a streamlined view of the unique features of different synthesis techniques that have influenced the final characteristics of the BBP, hence enabling effective catalyst design.

1.1 Sources of BC

BC is a carbonaceous material that is generated through the pyrolysis of organic matter at high temperatures. Essentially, any type of organic waste can be utilized as feedstock to produce BC. Various sources, including agricultural waste, poultry waste, forestry waste, food scraps, fruit pits, and bagasse, have been used to produce BC of different qualities (Shaaban et al., 2018). In this context, our focus is on the two most significant forms of organic waste generated by humans, namely agricultural waste and poultry waste. Food waste is one of the largest types of waste produced in the world, where almost 50% of municipal solid waste is from food sources. With both agricultural and poultry waste being a large bulk in this, adding value and repurposing this waste would be an ideal solution in reducing the strain of waste management systems across the globe.

When considering agricultural waste as a potential source of feedstock for BC production, various physicochemical properties of the waste should be considered. Factors such as the cellulose content and presence of foreign substances (such as trace metals and inorganic materials) can greatly impact the final quality of the BC produced (Yaashikaa et al., 2020). Agricultural waste with high cellulose content, such as husk, grass, bagasse, straw, nutshells, and fruit peels from various types of organic matter, such as rice, wheat, and coconut, are ideal feedstocks to produce BC. BC produced from such organic waste exhibits favourable characteristics that can be used for water remediation in integrated wastewater treatment systems through adsorption, as it has a large surface area, functional groups, and a high number of adsorption sites due to its porous nature. Furthermore, BC can be easily obtained via straightforward processes. This is especially true for husk and straw obtained from the production of rice and wheat, respectively, which are the two largest forms of carbohydrates consumed by humans on earth. Numerous research studies have demonstrated the potential of BC produced from rice husk (RH) and wheat straw (WS) in wastewater remediation. For instance, Hossain et al. prepared BC from RH via hydrothermal carbonization for wastewater remediation. The BC from RH exhibited a yield of almost 60%, and its high porosity and presence of SiO_2 significantly improved the material's adsorption efficiency of transitional dyes (Hossain et al., 2020). Another example of using agricultural waste to produce BC for

wastewater treatment is demonstrated by Tariq et al., who used wheat straw as a precursor to produce BC capable of adsorbing textile dye from wastewater by 62% (Tariq et al., 2022). The BC also reduced both chemical oxygen demand (COD) and biochemical oxygen demand (BOD) of treated water to permissible levels set by the Department of Environmental (DOE) in Pakistan (Hossain et al., 2020).

The poultry industry is another significant and growing industry due to the increasing demand for food worldwide. The growth of the poultry industry has been consistent globally, and it is expected to have a compounded annual growth rate (CAGR) of more than 10% for the next decade due to the increasing consumption and population growth (Kanani et al., 2020). The poultry industry, particularly in chicken, cow, pig, and goat rearing, has experienced significant growth, resulting in an increase in poultry waste production. Various types of organic waste can be found in the poultry industry, including livestock manure, poultry litter, dissolved air flotation (DAF) sludge from poultry processing plants, composts produced from hatchery wastes, and dead birds. Additionally, beddings used in poultry operations, such as wood shavings, sawdust, straw, feathers, feed spillages, and dead animals, can also serve as a source to produce BC. BC produced from the poultry industry differs from that produced from plant waste, with higher nitrogen and phosphorus content, cation-exchange capacity, adsorption capacity for metal ions, and ash content (Draper and Tomlinson, 2012). Furthermore, the presence of minerals such as nitrogen and phosphorus is also advantageous when developing BBP, as these minerals can serve as co-dopants along with BC to further optimize catalyst efficiency by improving the adsorption capacity and photoactivity of the catalyst (Lee and Park, 2020). However, the content of nitrogen and phosphorus in the prepared BC, especially in agricultural biomass is very small (less than 1%). While the phosphorus content in poultry biomass such as manure can be as high as more than 30%, the pyrolysis process which converts the biomass into BC effectively reduces the presence of phosphorus in the final product. Literature does present some papers that use a self-doping technique to prepare biochar-based materials self-doped with nitrogen and phosphorus. In cases where self-doping is mentioned, additional dopants are typically added to further enrich the nitrogen and phosphorus content for effective doping (Mian et al., 2018; Sutar et al., 2022).

1.2 Preparation of BC

As the interest in using BC as a sustainable substrate and dopant for photocatalyst development continues to grow, the techniques used to produce BC play a critical role in the quality of the

final product. Thermochemical conversion is a common method used to convert different biomasses into BC. Thermochemical conversion has consistently shown to produce biooils as well as BC with high yield conversion as well as being a mature reaction process. Several techniques are used in thermochemical conversion, including pyrolysis, hydrothermal carbonisation, gasification, and torrefaction. The selection of the method used to produce BC is based on the physicochemical properties of the biomass used, which will affect conditions such as the heating rate, residence time, maximum temperature, and other factors (Pan et al., 2021). Table 1 presents the various thermochemical conversion techniques that are used to convert biomass into BC. It is crucial to optimize these techniques to ensure that the maximum amount of BC can be extracted while maintaining desired quality.

Table 1 Thermochemical Conversion Processes for Biomass to Biochar (BC)

Technique	Temperature Range (ºC)	Residence Time	BC Yield (%)	By-products	BC Properties	Ref.
Pyrolysis	300 to 700 (slow)	Less than 2s	35	Bio oil & syngas	High yield of BC, high hydrophilicity, high ion exchange capacity	(Yaashikaa et al., 2020, Wang et al., 2014)
	500 to 1000 (fast)	1 hr to 24 hr	12	Bio oil & syngas	Higher surface area (>500 m^2/g), large porosity, high hydrophobicity	(Kruusenberg et al., 2021)
Hydrothermal carbonisation	180 to 300	1 to 16 hr	Up to 80	Bio oil & syngas	Higher surface area (>500 m^2/g), more aromatic and aliphatic functional group	(Kim et al., 2015)(Hossain et al., 2020)
Gasification	750 to 900	10 to 20s	10	Bio oil & syngas	Higher surface area (>500 m^2/g), meso and microporous structure, highly crystalline	(Muvhiiwa et al., 2019)
Torrefaction	290	10 to 60 min	80	Syngas	Lower hydroxyl functional group, lower surface area (<500 m^2/g), more stable	(Khairy et al., 2023)

When it comes to developing heterogeneous photocatalysts, certain physicochemical properties are highly desired in the substrates as they have been found to enhance photoactivity. These include having a high surface area, high porosity, carboxyl functional groups for anchoring, and a porous network. Based on these desirable properties, BC produced via pyrolysis (both slow and fast) is considered to be the one of the best quality of BC used as a substrate. Chatterjee et al produced BC through pyrolysis at 700 ºC has microporous structures and a surface area of nearly 200 m^2/g, which is above average . (Chatterjee et al., 2020). This is significant because traditional titania-based photocatalysts have an average surface area of between 40 to 60 m^2/g (Chatterjee et al., 2020; Youssef et al., 2018). The elevated treatment temperature effectively exfoliated the graphitic clusters within the prepared BC. This removed mineral matter and created openings in the structure, resulting in more significant microporous structures (Tomczyk, 2020). The high treatment temperature has the ability to decompose organic matter to a significant extent, which cannot be achieved with lower temperature treatments. However, increasing the treatment temperature further may lead to an unfavourable situation where the number of carboxylic functional groups decreases. These functional groups are important in bridging the substrate and metallic catalyst when developing BC-based photocatalysts. Higher temperatures (above 600 °C) can also result in the appearance of basic functional groups, highly aromatic, and well-organized carbon layers. These physicochemical structures may not be favourable in precipitating photocatalyst on the surfaces and pores of the BC. Poor interaction between the catalyst and the BC prepared may result in catalyst leaching. In addition, this set of physicochemical properties is also a result of the destruction of aliphatic alkyls and ester groups, as well as the exposure of the aromatic lignin cores to high pyrolysis temperatures (Tomczyk, 2020). Other methods listed in the table, including hydrothermal carbonisation and torrefaction also have elucidated the ability to produce BC of great quality with a higher yield percentage compared to pyrolysis. However, pyrolysis holds several advantages over the previously mentioned methods, including its shorter reaction time and the ability to produce solid based products (BC and biofuels) that can be easily transported as compared to gaseous products. The relatively lower temperature as well as shorter reaction time is imperative to reduce the energy expended for the production of BC and biofuels to improve the sustainability of the process.

2.0 Using BC as a substrate for developing photocatalysts

BBP are photocatalysts that use BC as a substrate and electron sink for visible light photocatalytic activation. While BC themselves do not exhibit any photocatalytic activity, pairing them with semiconducting materials such as TiO_2 and ZnO can impart these characteristics upon them. Such composite catalyst can be prepared using various methods and can be used to non-selectively photodegrade pollutants found in various wastewaters, including NOM, dyes, pharmaceutical compounds, and more. The performance of the photocatalyst in degrading these pollutants depends on several factors, including surface area, band gap, recyclability, and recombination rates, which are highly influenced by the synthesis technique used to develop the BBP. The most common synthesis techniques which are found in literature include sol-gel, co-precipitation, solvothermal, hydrolysis, and self-assembly. All the techniques mentioned above uses some form of metal precursors to grow the nanomaterials on the surface of the BC prepared. Various methods have been implemented in the literature over the years, as shown in Figure 2. Table 2 summarizes the development of BBPs using various techniques and their performance in remediating different pollutants.

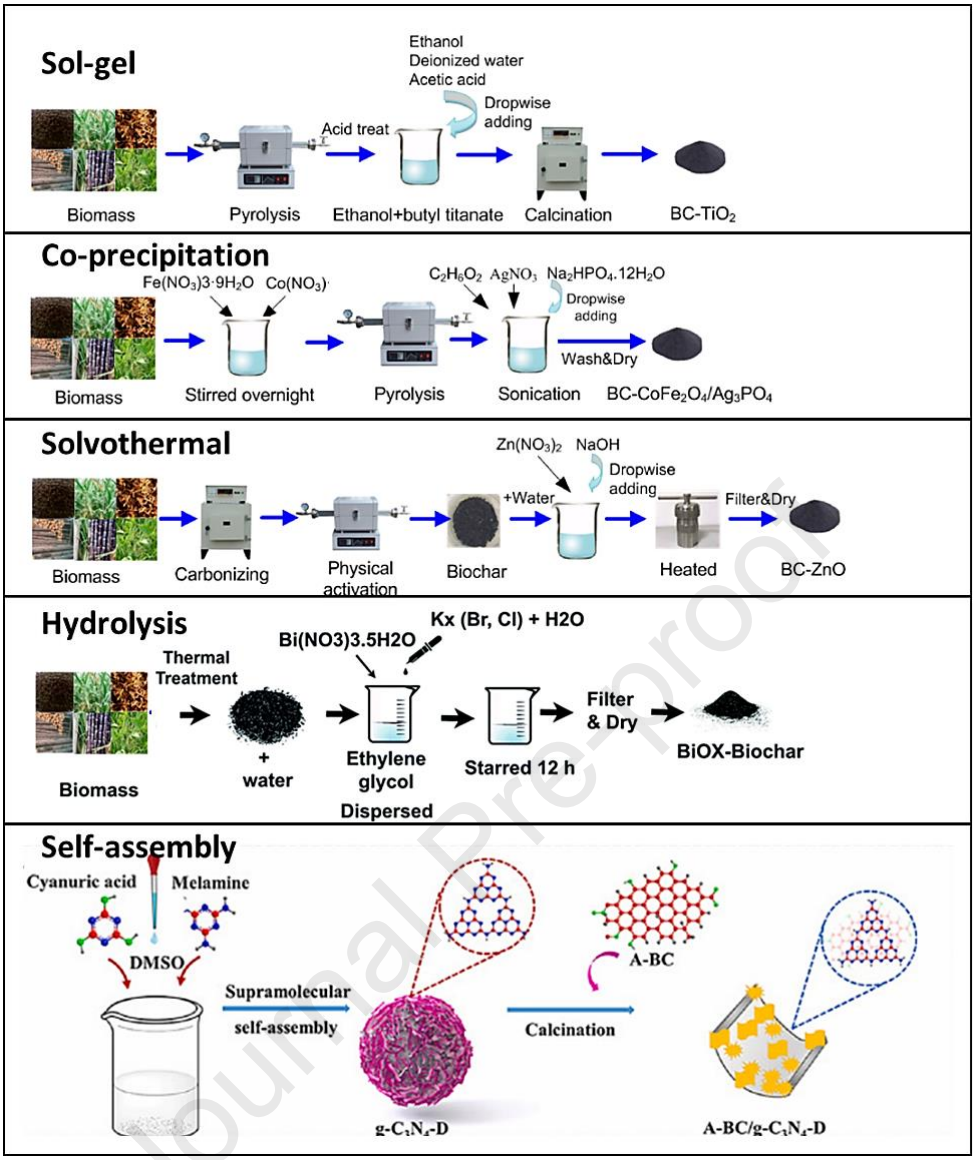

Figure 2 Synthesis Mechanisms for Various Techniques in BBP Development (Mian and Liu 2018)

Table 2 Comparison of Synthesis Routes and Performance of Various BBP Types

BBP	Biomass	Synthesis Technique	Band Gap (eV)	Pollutant	Removal (catalyst dosage, g/L)	Ref.
Cu–Fe–ZnO/BC	Anaerobic sludge	Co-precipitation	2.74	1,4 dioxane	93.1% (0.6)	(Samy et al., 2023)
Cu_2O-BC	Spent coffee ground	Co-precipitation	1.52	sulfamethoxazole	93% (2.0)	(Zheng et al., 2022)
ZnO-BC	Spent coffee powder and chitosan	Co-precipitation	3.31	methylbenzotriazole	99% (0.5)	(Gonçalves et al., 2022)
MnO_2-BC-C_3N_4	Cellulose fiber	Co-precipitation	1.09	Formaldehyde	91.78% (0.5)	(X. Li et al., 2022)
BC-ZnO	*Calotropis gigantea* (CG) leaves	Wet precipitation	2.97	ciprofloxacin	98.5% (1.0)	(Amir et al., 2022)
Ag_3PO_4/polyaniline/ BC	Waste tobacco stems	Chemical precipitation	2.34	Triclosan	85.2% (0.4)	(Ma et al., 2022)
Porous BC- Ag_3PO_4	Bamboo	*In-situ* precipitation	1.99	Methylene Blue	95.6% (0.5)	(Wei et al., 2021)
BC- $BiVO_4$	Walnut shells	Hydrothermal synthesis	2.00	4-aminobenzene sulfonamide,	97.0% (1.0)	(Zhang et al., 2021)
BC- $BiVO_4$	Korshinsk pea shrub	Ultrasonicationand hydrothermal synthesis	2.26	rhodamine B tetracycline, norfloxacin, chloramphenicol	73.5% to 99% (1.0)	(Wang et al., 2022)
α-$NiMoO_4$/$ZnFe_2O_4$/BC	Spent ground coffee	Hydrothermal synthesis	2.17	ketoprofen	99% (1.0)	(Kumar Ray et al., 2023)
BC-$PbMoO_4$	Poplar sawdust	Solvothermal and pyrolysis	2.59	Tetracycline	61.0% (3.0)	(Chen et al., 2021)

TiO_2-BC	cornstalk powder	Thermal synthesis	>3.2	*E.coli*	>90% (1.0)	(Xie et al., 2022)
Mesoporous TiO_2/CS-BC	chitosan	Solid phase co-calcination and sol-gel	>3.2	Rhodamine B	>98% (0.5)	(Feng et al., 2022)
BC- $ZnFe_2O_4$	chitin	Sol-gel	1.67	Rhodamine B	100% (20.5 to 2.0)	(Welter et al., 2022)
BC/TiO_2	Peanut sell	Sol-gel	>3.2	Methylene Blue	90% (0.3)	(Luo et al., 2022)
BC-Fe@Persulfate	Black seed pomace	Wet impregnation	<3.2	Rhodamine B	98.2% (1.5)	(Mustafa and Hama Aziz, 2023)

2.1 Sol-gel

The sol-gel technique is commonly used in synthesizing semiconductor photocatalysts using precursors. This method enables the preparation of different photocatalysts in various shapes on the surface of BC via impregnation. For instance, Zhang et al. used TiO_2 as the photocatalyst of choice in preparing a BBP via sol-gel impregnation for the remediation of sulfamethoxazole in aqueous matrices (Zhang et al., 2017). Hydrochloric acid was utilized to eliminate impurities of BC, which was then soaked in absolute ethanol, tetrabutyl titanate and acetic acid. The resulting sol was left to age for two days and then calcined at 500°C in a muffle furnace for 2 hr to complete the synthesis. Meanwhile, Cai et al. opted to use titanium butoxide as precursor to cultivate Ti nanoparticles on BC produced from ramie bar (Cai et al., 2018). Although similar precursor has been used, the BBP produced in this work is smaller than that of reported by Zhang et al. The size variance indicates the flexibility of sol-gel technique which provides avenue to use different precursor material in regulating the size of BBP. The size of the BBP produced in this work was about 27.53nm, while in Zhang et al.'s work, the size of the BBP was 34.7 nm. The size variance indicates the flexibility of sol-gel technique in regulating the size of BBP. Catalysts of uniform size, particularly smaller ones, consistently demonstrate better photoactivity efficiency than uncontrolled and larger-sized catalysts. The larger number of active sites on the surface and faster spatial charge transfer are two significant advantages of size-controlled catalysts (Li et al., 2020). Lee et al. utilized the same sol-gel technique to prepare TiO_2 BBP using rice husk BC, to remediate glyphosate in aqueous conditions (Le et al., 2021). Here, the researchers used titanium tetraisopropoxide (TTIP) as the precursor to produce TiO_2 BBP using rice husk BC through the sol-gel technique for the remediation of glyphosate in aqueous conditions. The resulting particles had a reported size of 40 nm.

2.2 Co-precipitation

Co-precipitation is a commonly used method for producing bimetallic or multi-metallic nanomaterials and is highly effective for tuning and yielding high percentages of photocatalyst. Leichtweis et al. utilized this technique to develop a BC-based $CuFe_2O_4$ photocatalyst for the degradation of rhodamine B (RhB), a potent textile dye (Leichtweis et al., 2021). Malt-derived BC was used as a substrate to grow copper and iron nanoparticles on its surface using co-precipitation technique. The BC was produced through pyrolysis at 350°C under N_2 atmosphere for 1 hour and then ground into a 30-mesh screen. Iron and copper nitrate were mixed and added to the prepared BC, followed by pH adjustment to 11-12 and heating at 80°C

for an hour to form the composite photocatalyst. The sample was rinsed with distilled water to remove any unreacted ions, dried, and ground for photocatalytic testing. The characterization of the photocatalyst showed that the band gap was reduced from 1.9 eV to 1.23 eV. This method produced a highly efficient photocatalyst for the remediation of rhodamine B (Cufe and Liu, 2019). Zhang et al. also used a similar approach, where they mixed calcium and tungsten precursors with BC, adjusted the pH to 10, and dried the mixture at 50 ºC (Zhang et al., 2019). According to reports, the co-precipitation technique enables the precursor solution to enter the porous structure of BC, thus initiating the formation of nuclei for nanoparticle growth, increasing the active sites for nanoparticle formation. This led to the growth of nanoparticles on the surface and inside pores of BC, utilizing BC as a growth template. Similarly, Chen et al. developed a BC-based ZnO photocatalyst for the photodegradation of methylene blue (MB) dye (Chen et al., 2019). Here, the growth of photocatalyst occurred simultaneously with the conversion of biomass into BC. Jute sticks were soaked in zinc acetate dihydrate (precursor), and then the sample was transferred into a crucible to remove moisture and carbonized at 700 ºC for 2 hr at a heating rate of 5 ºC/min. Impregnating the photocatalyst precursor before carbonization allowed the interaction between zinc and carbon in the biomass to determine the size of particles produced during carbonization. Co-precipitation is not only used to grow one or more metal nanoparticles on templates but also provides a feasible way to incorporate more than one substrate material, as demonstrated in the work by Gonçalves et al.(Gonçalves et al., 2022). In this study, the researchers used brewed coffee waste and chitosan to produce BC, which was then incorporated with different loadings of ZnO particles via co-precipitation technique. To produce the BC, both brewed coffee waste and chitosan were washed with deionized water and dried at 105 ºC for 72 hr, followed by pyrolysis at 800 ºC under argon atmosphere for 30 min. The BC was then oxidised to improve the BC-metal interaction. The oxidised BC was soaked in acetic acid before being used as a template in co-precipitating ZnO particles. It was found that the oxidised BBP exhibited a higher amount of ZnO particles incorporated compared to the non-oxidised BBP.

2.3 Solvothermal

This method involves mixing the biomass in ethanol and adding a metal precursor, followed by high temperature and pressure treatment in an autoclave, washing, filtration, and drying. The final step is thermal treatment in a furnace before the BBP is ready for characterization and performance evaluation. Chen et al. used this method to prepare a BBP photocatalyst using a combination of Zn, Fe, Bi, and Br for the treatment of ciprofloxacin under visible light

conditions (Chen et al., 2019). In this study, BC@$ZnFe_2O_4$ was first prepared by precipitating $K_2Fe_2O_4$ and $n(CH_3COO)_2 \cdot 2H_2O$ onto pine pollens. The resulting samples were then subjected to hydrothermal condensation (at 160 ºC for 12 hr) in a Teflon-lined autoclave to incorporate both Bi and Br, thus producing a heterojunction BBP. The addition of BiOBr lowered the BBP's band gap from 2.87 eV to 2.02 eV, and when tested for its optical properties, a visible red shift (from 559 nm to 446 nm) was observed in the adsorption edge.

2.4 Hydrolysis

Researchers commonly use a simple hydrolysis technique to improve the visible light sensitivity of various photocatalysts. Xie et al. developed a magnetic Fe_3O_4/BiOBr/BC through a modified one-step hydrolysis technique to treat carbamazepine in aqueous conditions (Xie et al., 2021). The synthesis method involved adding the desired precursor to ethylene glycol, which was then alkalized with NaBr and mechanically stirred to produce the BBP. The addition of Fe and BC carbon sources improved visible light absorption, leading to increased photogenerated charge separation. This was confirmed by XPS analysis which showed interaction between Fe and C. The synergistic interaction between Fe, C, and Bi led to the formation of a heterojunction photocatalyst that exhibited remarkable removal efficiency of carbamazepine, with up to 95% being removed within 3 hr. In another study, Reguyal et al. grew Fe on BC derived from pine saws to prepare a magnetic pine saw BC (MPSB) for the removal of sulfamethoxazole under aqueous conditions (Reguyal et al., 2017). $FeSO_4$ was hydrolysed in an alkali media solution (3.33 M KOH and 0.27 M KNO_3) in the presence of BC particles. The resulting sample was sealed, cooled overnight, and centrifuged before being washed and dried. The sample had a high surface area of 125.8 m^2/g, indicating a high number of active sites available for adsorption. The magnetic properties of the sample allowed for easy recyclability after heterogeneous adsorption of sulfamethoxazole. The Fe_3O_4 nanoparticles on the surface of BC contributed to a high saturation magnetisation of MPSB, 47.8 A m^2/kg, enabling its separation from aqueous solution using a magnet. The prepared sample exhibited high adsorption efficiency towards sulfamethoxazole

2.5 Self-assembly

In order to achieve greater control in the design of photocatalysts, researchers have turned to the self-assembly technique. This technique involves using basic units that interact cooperatively to form the catalyst, allowing for more precise control over its formation compared to other methods used for multi-component catalysts. Lin et al. applied this technique

to develop a BC-based supramolecular self-assembled g-C_3N_4 for improved visible light photocatalytic degradation of phenanthrene in aqueous conditions (Lin et al., 2022). The self-assembly technique requires the use of BC as both the substrate and composite material for the catalyst. The BC is placed in a KOH solution to produce a KOH-modified BC that increases the reactive sites on the BC. The KOH-modified BC and g-C_3N_4 are then ultrasonicated and heated in the presence of water, dried, and calcined at 450 ºC for 2 hr. The self-assembly technique facilitates thermal polymerisation of g-C_3N_4 on the BC, forming a complex hollow and porous structure. This enhances the photoactivity of the g-C_3N_4 due to the increased active sites. Additionally, a π-hybrid conjugated structure is formed between g-C_3N_4 and BC. Li et al. also used the self-assembly technique to prepare a BBP by adding TiO_2 and graphene as composite materials (Li et al., 2018). In this study, KOH was used to activate more sites for the composite materials to anchor on, using the self-assembly technique. The resulting photocatalyst exhibited interactions between Ti-O and the C from BC, which created electron transport channels that enhanced visible light sensitivity. The TiO_2-graphene BBP also demonstrated the ability to degrade over 90% of the target pollutant (RhB) in just 4 hr.

3.0 Role of BC in enhancing photocatalytic performance

The sustainable nature, low production cost, and abundance of BC make it an ideal material for developing heterogeneous photocatalysts for environmental remediation, particularly in wastewater treatment. The microporous structure, large surface area, and surface functional groups present in BC make it an ideal substrate for hosting metal photocatalysts, increasing the affinity of pollutants with the photocatalyst through a larger number of active sites and porous channels, resulting in more efficient pollutant remediation. The addition of BC to photocatalysts has been shown to improve their ability to degrade various types of organic pollutants in aqueous conditions.

3.1 Reducing bandgap

Researchers initially explored the use of BC in developing photocatalysts because BC can serve as a dopant that imparts visible light sensitivity to traditionally UV-responsive photocatalysts. Dopants are incorporated with photocatalysts for several reasons, such as enhancing the photocatalytic rate by reducing recombination rates, providing an electron sink to sustain longer photocatalytic activity, and providing an alternate pathway for electron movement to enhance photocatalytic reaction rates (Nair et al., 2022). Typically, titania-based photocatalysts

have a band gap in the range of 3.1-3.2 eV, which is significant because a band gap of more than 3.0 eV is considered to be in the UV region for photoactivation (Nair et al., 2022). UV-Vis light absorption originates from the electron transmission from the valence band to the conduction band, whereas the band gap is defined by the distance between the valence and conduction bands, which is regulated by the ratio of the doping agent. The valence band (VB) of TiO_2 is formed by the hybridization of 2p orbitals of O_2 and 3d orbitals of Ti, and the conduction band (CB) comprises pure 3d orbitals of Ti (Hu et al., 2020). Therefore, traditional titania-based photocatalysts require UV light sources to achieve the necessary energy to be activated ($\lambda \leq 390$ nm). This is where dopants can play a significant role. Doping titania photocatalysts with the carbon present in BC reduces the band gap energy value due to the formation of new energy levels near the conduction band. The carbon present in BC is mainly incorporated interstitially, which narrows the bandgap, resulting in a red shift in the UV-visible (UV-vis) spectrum and an increase in adsorption of near-infrared (NIR) spectrum. This shift allows the photocatalyst to be activated in the visible light region (400–700 nm). The incorporation of carbon can also lead to defects, where dopant atoms occupy Ti sites or interstitial sites, which can also impact the final band gap energy of the prepared photocatalyst.

3.2 Electron Sink

Carbon-based materials such as graphene oxide, carbon dots have been extensively researched as dopants to enhance photoactivity. Recently, BC has been of a particular interest among researchers. BC has shown promise and evidence that it possesses electron storage capacity (ESC), allowing it to store and reversibly exchange electrons with its environment. The ESC and exchange efficiency are influenced by BC processing parameters, such as the source of biomass used for production and pyrolysis temperature. Xin et al. investigated the ESC of BC produced from feedstocks rich in cellulose, xylan, lignin, wood, and a mixture of different biopolymers and how different pyrolysis temperatures affect them (Xin et al., 2021). The results indicated that pyrolysis at temperatures above 450 °C resulted in BC with a highly reversible ESC of 1-2 mmol e^-/g from lignocellulosic biomass. This ESC was likely created by converting oxygen-containing moieties of the biopolymers into (hydro)quinones in BC during pyrolysis. Different biomass sources heated at different temperatures undergo various transformations, which affect the molecular mechanism of ESC creation. Furthermore, Xin et al. used silver tagging to investigate the distribution of ESC on BC and found that a significant portion of ESC was located in the interior of wood BC (Xin et al., 2020). Similar to graphene, layered BC has higher electron conductivity compared to stacked BC due to the increased

availability of localized electrons. This suggests that cleavage and exfoliation of BC may be necessary to improve its ESC when used as a dopant in photocatalysts. The spatial distribution of ESC also plays a role in the bioaccessibility and redox reaction rates of BC.

3.3 Increasing surface area

The redox reaction during photocatalysis occurs on the surface of the photocatalyst. Most prepared photocatalysts have a low surface area, typically ranging from 10 to 60 m^2/g, depending on factors such as structure, shape, and porosity (Dharma et al., 2022). However, BCs are known to have a porous structure, providing a large surface area. Additionally, they contain abundant oxygen functional groups, an aromatic surface, and high porosity. When photocatalysts are dispersed or grown on the surface of BC, they can greatly increase the overall surface area of the composite photocatalyst compared to non-BC photocatalysts. Suitable immobilization techniques can lead to the development of composite photocatalysts that provide numerous active sites for enhanced redox reactions. This can also improve the dispersion of photocatalysts in heterogeneous reactions and improve light scattering. For example, Wang et al. modified BC with TiO_2 using the wet impregnation technique for the removal of enrofloxacin (Wang et al., 2020). The results of the BET analysis showed that the specific surface areas of BC, Ti-BC, Ti-FBC, and Ti-KBC were 15.24, 36.65, and 40.46 m^2/g, respectively. Compared to BC, Ti-BC, Ti-FBC, and Ti-KBC possessed surface area that is 4.34, 10.43, and 11.52 times higher, respectively. Alkali treatment was used to increase the surface structure and the number of micropores, which is a common technique used to enhance BC surface area before impregnation of photocatalyst (Liang et al., 2022; Liu et al., 2020). Hosseini-Monfared et al. conducted research on utilizing BC as a substrate for nitrogen-doped TiO_2 photocatalyst, using a combination of sol-gel and thermal synthesis techniques (Hosseini-Monfared et al., 2021). The findings showed that the addition of N-TiO_2 to BC improved its ability to adsorb substances, and the large specific surface area of BC boosted the photocatalytic performance of N-TiO_2. The synthesis method also influenced the findings, as using urea as the nitrogen source created defects in the structure, increasing the surface area even more. However, it was found that heating the samples to 500 °C during the preparation process could cause the pore structure in the BC to collapse, reducing its overall surface area and porosity.

3.4 Improving charge separation/recombination

One important factor that significantly impacts the photoactivity of a photocatalyst is the rates of charge separation and recombination. Essentially, charge separation occurs when an electron is excited from a lower energy level to a higher one. During this process, the electron departs from the atom, leaving it positively charged and generating an electron-hole pair. This, in turn, enables the production of radical species. Figure 3 illustrates the process of electron excitation and demotion during photoactivity.

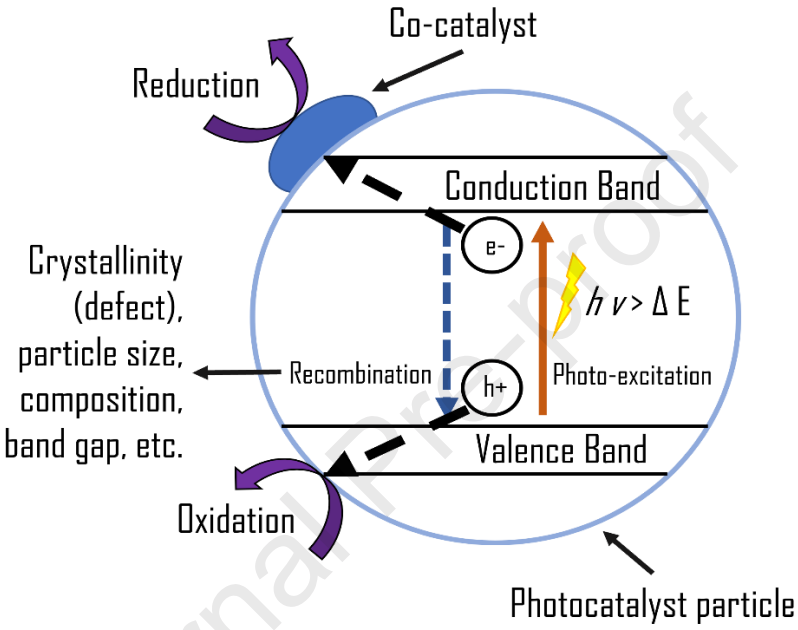

Figure 3 Charge Separation and Recombination in Photocatalyst Activation under Irradiated Light

When examining charge separation and recombination more closely, three mechanisms are typically used to describe the charge separation process: built-in electric field, diffusion, and trapping (Shishido et al., 2011). Among these, built-in electric field is considered the most frequently occurring driving mechanism of charge separation for heterojunctions, phase-junctions, and crystal-facet engineering. Researchers have conducted studies to gain a better understanding of how photogenerated charges are distributed across various catalyst types, such as n-type $BiVO_4$ and p-type Cu_2O (Chen et al., 2022). Surface photovoltage microscopy (SPVM) images have revealed that charge separation takes place on the surface of particles. This suggests that the built-in electric field in the surface space charge region facilitates charge separation between the surface and bulk phase of a photocatalyst. This electric field is caused by the bending of the surface band of semiconductors. An upward bend leads to the formation of n-type semiconductors, while a downward bend results in p-type semiconductors. This

means that the distribution of charges is closely linked to the surface built-in electric field. Modifying the surface of a photocatalyst, such as by increasing its surface area or introducing specific functional groups, or adding electron sinks to the surface, can all be crucial in enhancing charge separation and reducing recombination rates to improve photoactivity.

4.0 BC based photocatalytic degradation of POPs

4.1 Photocatalytic reaction mechanism

Before we explore the effectiveness of different BBP for photodegradation in remediating various organic compounds, it is necessary to discuss the basics of photodegradation mechanisms exhibited by the use of such BBP. The inclusion of BC in the photocatalyst composite significantly affects the band gap, electron movement, and activation energy required. Figure 4 illustrates the photocatalytic activation mechanism of a TiO_2-BC BBP in degrading organic pollutants.

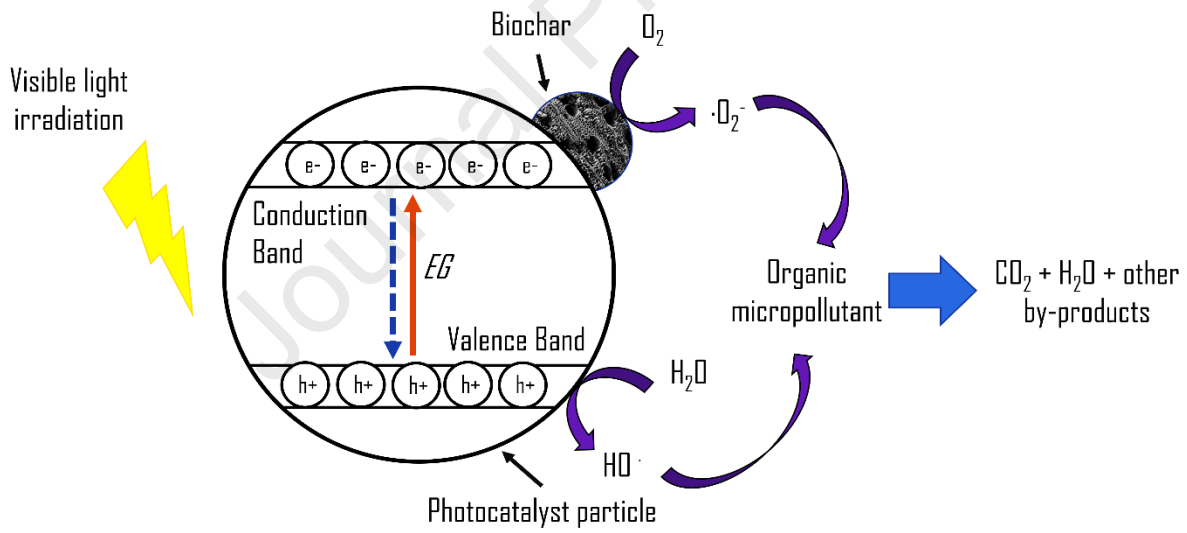

Figure 4 Photocatalytic Degradation Mechanism of TiO_2-BC Composite for Organic Pollutant Remediation

Eq.	Reaction	
1.0	Photo-excitation	$TiO_2 \xrightarrow{hv} e^- + h^+$
2.0	Recombinatoin	$e^- + h^+ \longrightarrow$ heat
3.0	Reduction	$O_2 + e^- \longrightarrow O_2^-$
4.0	Redox reactions	$O_2^- + HO\cdot \longrightarrow HOO\cdot$

4.1 $HOO^{\cdot} + e^{-} \longrightarrow HO_2^{-}$

4.2 $HOO^{-} + H^{+} \longrightarrow H_2O_2 \longrightarrow HO^{\cdot}$

4.3 $H_2O \longrightarrow H^{+} + OH^{-}$

4.4 $OH^{-} + h^{+} \longrightarrow HO^{\cdot}$

When a catalyst absorbs photons, *hv*, with energy equal to or greater than its band gap, its photocatalytic activity is activated. As shown in Figure 4, the absorbed energy excites an electron from the valence band to the conduction band. This movement generates an electron-hole pair phenomenon, where both the electron and hole concurrently conduct oxidation and reduction reactions with any organic material present, including water and pollutants. The reduction of water results in the formation of reactive oxidative species (ROS), which are non-selective radicals that react with organic matter, as seen in Eq. 4.0 to 4.4. When the energy is depleted, the electron falls back into the valence band and becomes inactive, which is called recombination. This excitation and deactivation cycle occurs repeatedly as long as photons are available for adsorption. The presence of BC in the composite material brings about significant changes in this process, including a lower band gap value and a longer pathway for the electron to return to the valence band (Gao et al., 2019). Doping a photocatalyst with BC results in a lower band gap value, which reduces the energy required to initiate photoactivity (Hu et al., 2017). If the band gap of a photocatalyst is 3.2 eV (TiO_2), it would need light sources in the UV region (< 400 nm) to be activated. However, doping the catalyst results in a lower band gap (< 3.2 eV), allowing it to be activated by longer wavelength light sources, including the visible light range (> 400 nm). Furthermore, the presence of BC with available localized electrons functions as an electron sink (Sathishkumar et al., 2020). After electrons expend their energy during the excitation stage, they do not immediately return to the valence band but instead move momentarily into the electronic structure of BC. This results in an increased lifespan of the hole, allowing for a greater number of produced ROS. The delay in electron return also slows down the recombination rate of the electron-hole pair (Qian et al., 2019). All of these changes result in an increase in ROS availability, which directly enhances the rate of photodegradation and overall photoactivity.

4.2 Pharmaceutical Waste

The healthcare industry's growth in recent decades has significantly improved people's quality of life. However, one downside of this expansion is the identification of various contaminants

in pharmaceutical products, which can harm people's health. The unregulated and illicit release of wastewater from the pharmaceutical industry has resulted in the detection of pharmaceutical active compounds such as antibiotics, anti-inflammatory compounds, and compounds that mimic human hormones. These compounds are known to be harmful to the human body (Rosman et al., 2018). Bioaccumulation of such compounds into the human body can lead to various short- and long-term health implications (Eniola et al., 2022). Photocatalysis has great potential for removing harmful contaminants from wastewater in an environmentally friendly way. By combining photocatalysts like TiO_2 and ZnO with BC, the number of active sites can be increased, the band gap can be lowered, and the sensitivity to visible light can be enhanced. The effective surface area of the resulting BBP can vary from 45 m^2/g to 520 m^2/g, indicating that factors like processing temperature, exfoliation, and synthesis technique are important in determining the final characteristics of the BBP. In addition, incorporating BC into BBP can decrease the band gap and enable activation with visible light sources like xenon and LED lamps. Table 3 compiles various studies on the development of BBP for the photodegradation of pharmaceutical compounds found in water streams, including ciprofloxacin, triclosan, tetracycline, sulfamethazine, ofloxacin, and gemifloxacin.

.

Table 3 Utilization of BBP for Pharmaceutical Wastewater Remediation

BC composite	**BC source**	**Surface area (m^2/g)**	**Light source**	**Pollutant**	**Major Reactive species**	**Removal % (loading)**	**Recyclability**	**Ref.**
BC-ZnO	*Calotropis gigantea* leaves	-	LED lamp 3 W	ciprofloxacin	OH• and $O•_2^-$	98.5% (1.0)	80.3% (4^{th} cycle)	(Amir et al., 2022)
BC-TiO_2	Rice straws	47.37	-	ciprofloxacin	OH^-	83.8% (0.5)	-	(Qu et al., 2023)
$BiVO_4$@N-BC	Aspen wood chip	20.04	Xe lamp (250W)	triclosan	•OH, O_2•- and h^+	72.3% (0.1)	88.1% (4^{th} cycle)	(Wei et al., 2022)
ZnFe-layered @ BC	Rice husk	79.2	LED lamp (5W)	tetracycline	•OH, O_2•- and h^+	87.7% (2.0)	81% (3^{rd} cycle)	(M. Li et al., 2022)
MoS_2/S,N-BC	Chitosan	384.71	Xe lamp (300 W)	tetracycline hydrochloride	•OH and OH−	99.3% (0.4)	93.4% (5^{th} cycle)	(Peng et al., 2023)
BC	Swine sludge	56.78	Hg lamp (4 W)	sulfamethazine	•OH and h^+	91.5% (1.0)	88.0% (5^{th} cycle)	(Ke et al., 2022)
$LaFeO_3$-BC	Lignin	52.529	Xe lamp (300 W)	ofloxacin	•OH, h^+, $•O_2–$, $^1O_2$	95.6% (0.25)	91.9% (5^{th} cycle)	(X. Chen et al., 2022)
MnFe-LDO–BC	Palm seeds	524.8	UV 9–30 W	tetracycline	O_2•– and h^+	98% (1.0)	80% (3^{rd} cycle)	(Azalok et al., 2021)
Zn-Co-LDH@BC	Wheat husk	112.93	UVB 10 W	gemifloxacin	•OH	92.7 % (1.0)	82% (5^{th} cycle)	(Gholami et al., 2020)

In the field of wastewater treatment, researchers have explored the use of BBP combined with various catalysts and different sources of BC to remove pharmaceutical compounds. Table 3 contains information on the different types of BBP that have been developed and successfully utilized for the remediation of various pharmaceutical compounds. The use of BC as a support and dopant for photocatalyst development has shown promising improvements, including the reduction of band gap energy for activation, inhibition of electron hole/recombination, a larger surface area for increased active sites, and improved adsorption and photocatalytic efficiency. These changes were observed in the work conducted by Qu et al., where rice straw was used to produce BC and subsequently employed as a substrate for TiO_2 in the photodegradation of ciprofloxacin, a broad-spectrum antibiotic (Qu et al., 2023). Researchers carbonized rice straw using a tubular furnace, then used it as a substrate for TiO_2 photocatalyst growth via co-precipitation with tetra-n-butyl titanate as a precursor. Microscopic imaging coupled with EDX analysis showed that the titanium (Ti) grew on the surface of the BC with good dispersion. BET analysis revealed that the surface area of TiO_2-BC was three times larger than that of BC only (47.4 m^2/g compared to 16.3 m^2/g), and the pore volume also increased (0.018 cm^3/g to 0.033 cm^3/g). Processing technique plays an important role in affecting the pore structure of BBP. Literature shows that most of the surface area value for BBP is owed to the porous nature of BC. Different processing techniques may act as exfoliation to further enhance the surface area value of BC. The co-precipitation technique uses phosphoric acid, which dissolves inorganic minerals inside the porous network of BC, exfoliating them to increase both pore size and volume. The growth of TiO_2 on BC also reduced the band gap of the catalyst to 2.15 eV, compared to 3.2 eV for undoped TiO_2. The increased surface area and lower bandgap jointly enhanced photoactivity, where the BBP degraded up to 84% of ciprofloxacin within 200 min.

Zinc oxide is another material that has been found to exhibit photoactivity and is typically combined with iron to create an active photocatalyst. However, similar to titania based photocatalysts, these are only activated under UV light. To address this limitation, researchers have also explored the co-synthesis of these photocatalysts with BC materials to create visible light active photocatalysts. This approach was successfully demonstrated in the work conducted by Li et al.(Li et al., 2022). The researchers developed ZnFe-layered double hydroxides @ BC nanocomposites through co-precipitation and hydrothermal synthesis for the degradation of tetracycline, a common antibiotic compound. The BBP had a relatively rough surface and irregular porous structure with some attached aggregates, possibly produced

through the formation of volatile substances during pyrolysis. The incorporation of BC in the composite allowed higher visible light absorption capacity, as evidenced by a red shift in the UV-Vis diffuse reflectance spectra. The spectra estimated that the band gap of the BBP was 2.38 eV, lower than that of the nanocomposite without BC, which was 2.59 eV. The addition of BC inhibited recombination of electrons and holes, leading to longer periods of photoactivity, as indicated by higher conductivity and stable photosensitivity seen in transient photocurrent responses. The BBP exhibited excellent stability, with the ability to degrade 95% of tetracycline within 130 mins of reaction time under visible range LED light and degradation efficacy of more than 85% even after three cycles in recycling tests.

In a study conducted by Gholami et al. (Gholami et al., 2020), a similar synthesis method was employed to create a BC-Zn-Co-layered double hydroxide photocatalyst for the photodegradation of gemifloxacin, a discontinued antibiotic compound. TEM imaging revealed that the co-precipitation of ZnCo nanoflake crystals on the BC surface led to significantly higher surface roughness compared to pristine BC. Surface analysis also showed that the incorporation of ZnCo nanoflakes with BC resulted in the development of a nanocomposite photocatalyst with a regular shape and improved specific surface area (95.76 m^2/g) compared to pristine BC (68.19 m^2/g). The Zn-Co-layered double hydroxide @ BC was capable of removing more than 92% of gemifloxacin within 100 min of photoactivation. The presence of both copper (Co) and BC as co-dopants prevented the fast recombination rate of photo-catalytically generated holes and electrons and prevented the aggregation of Zn-Co-LDH components. The study also indicated that hydroxyl radicals were the primary oxidising species generated to degrade gemifloxacin in these reactions. Furthermore, the stability test demonstrated that these BBPs were highly stable, as they were able to maintain more than 90% efficacy after five cycles of photodegradation. The results showed that BC played a dual role in enhancing photoactivity, providing a substrate for the development of a photocatalyst with a larger surface area, as well as facilitating lower combination rates by serving as an electron sink, thereby prolonging the period of electron hole pairs and generating a greater number of oxidising species.

Chen et al. (Chen et al., 2022) carried out research on the degradation of ofloxacin, a type of quinolone antibiotic, using lignin-based BC and $LaFeO_3$ BC composites as a source of heterogeneous photo-Fenton-like catalysis. The SEM and TEM images revealed that the lignin-based BC had an irregular flaky shape, while the LFO exhibited a larger agglomerated microsphere morphology. The unique flaky structure of the lignin-based BC prevented the

formation of bulky BC particles, leading to the creation of larger numbers of pores within the composite, allowing it to exhibit higher adsorption and photoactivity to ofloxacin. EDX analysis indicated that the LFO particles grew evenly over the BC flakes, while BET analysis showed that the surface area and porosity of the composite increased significantly compared to BC alone. Electronic properties analysis revealed that the band gap of the composite was within the visible light range, allowing it to be activated by visible light. Photocurrent analysis confirmed that photo-induced electron-hole pairs separation was longer, resulting in lower recombination rates. These improvements led to the effective photodegradation of ofloxacin, with more than 98% degraded within 80 mins. Additionally, toxicity analysis using fathead minnows and rats demonstrated that the degradation by-products were not toxic, unlike ofloxacin, which is known to be mutagenic to these organisms.

4.3 Phenolic compounds

Phenolic compounds are widely used in various industries, particularly in plastics and polymers. These materials include bisphenol-A and nitrophenol, which are used in the manufacturing of plastics, dyes, and rubber, as well as nonylphenol, which is essential in the production of antioxidants, lubricants, and laundry detergents. Unfortunately, the presence of these compounds in wastewater can have harmful effects on all living organisms, as some of them are known to disrupt endocrine function and mimic natural hormones. Due to the stability of phenolic compounds at temperatures up to 50 °C and their chemical resistance, researchers have become increasingly interested in developing efficient photocatalysts for their remediation. Table 4 provides an overview of recent research on the use of BBP for the removal of phenolic compounds.

Table 4 Utilizing BBP for the Remediation of Phenolic-Contaminated Wastewater

BC composite	**BC source**	**Surface area (m^2/g)**	**Light source**	**Pollutant**	**Major Reactive species**	**Removal % (loading)**	**Recyclability**	**Ref.**
Cu-Fe /BC/Ag_3PO_4	Pine needle leaves	163.86	Xe lamp (300W)	phenol	•OH and h^+	100% (1.0)	65.86% (5^{th} cycle)	(Liu et al., 2022)
ZnO-BC	Pomegranate peel	-	Natural sunlight	phenol	h^+	91% (1.0)	-	(Mankomal and Kaur, 2022)
BC@$CoFe_2O_4$/Ag_3PO_4	Pine pollen	14.973	Xe lamp (300W)	Bisphenol-a	h^+ and $•O_2^-$	91.12 (0.2)	73.94% (4^{th} cycle)	(Zhai et al., 2020)
Ag_3PO_4/Fe_3O_4-BC	Bamboo particles	4.28	LED lamp (250W)	Bisphenol-a	$•O_2^-$	95.6 (1.0)	70% (3^{rd} cycle)	(Talukdar et al., 2020)
Co-BiOCl/BC	Sedimentation tank sludge	-	Mercury lamp	Bisphenol-a	•OH, $•O_2^-$ and h^+	93.8 (-)	90% (5^{th} cycle)	(Cao et al., 2022)
BC templated C_3N_4/$Bi_2O_2CO_3$/$CoFe_2O_4$	pruning waste	68.24	Xe Lamp (800W)	Paraquat and nitrophenols	$•O_2^-$	84.5% (0.5) 99.3 (0.5)	98.1% (5^{th} cycle)	(Kumar et al., 2018)
BC-$CoFe_2O_4$	Peanut shell	93.8	-	nonylphenol	•OH, $^1O_2$ and $SO_4^{•-}$	90.6 (1.5)	>90% (5^{th} cycle)	(Song et al., 2023)
C_3N_4-BC	Corn cob	-	Xe lamp	Bisphenol a	•OH	83.7% (0.4)	-	(Wang et al., 2021)

In a recent study conducted by Mankonal and Kaur, the authors investigated the potential use of a ZnO nanoflower impregnated in BC derived from pomegranate peels for the photodegradation of phenol (Mankomal and Kaur, 2022). The synthesis method involved a chemical precipitation technique under low temperature (< 90 ºC), followed by processing with ammonia and pomegranate peel BC. The surface characterization of the resulting BBP indicated a unique flower-like architecture with nanorods of varying lengths (ranging from 150 to 850 nm) and nanopetals. EDX analysis revealed that the ZnO nanoflowers were well-dispersed on the structure of BC, making use of the large active sites available due to the porous nature of BC. The BBP was found to photodegrade 91.6% of phenol within 150 min of reaction time. However, it should be noted that approximately 55% of the removal was attributed to adsorption, indicating that both adsorption and photocatalysis could work together to remove phenol. The use of BC in this work enhanced the photoactivity of the BBP by reducing the band gap (<2.6 eV) and inhibiting electron-hole pair recombination, while simultaneously increasing the surface area of the material. These multi-faceted improvements highlight the potential benefits of utilizing BC in photocatalysts for the degradation of pharmaceutical pollutants such as phenol.

Liu and colleagues developed a photo-corrosion resistant photocatalyst, consisting of a heterojunction Cu-Fe/BC/Ag_3PO_4, to eliminate phenol from aqueous streams (Liu et al., 2022). The researchers utilized pine needles as the carbon source for BC preparation and employed hydrothermal technique and in-situ precipitation to develop the heterojunction photocatalyst. TEM imaging revealed that the irregularly shaped BC and spherical Ag_3PO_4 were dispersed on the surface of the regular polyhedron $CuFe_2O_4$, forming a composite structure that facilitated the formation of heterojunctions. The surface area of the composite structure increased to 163.86 m^2/g due to the incorporation of BC, compared to only 31.45 m^2/g for $CuFe_2O_4$. Photoluminescence spectra demonstrated that the fluorescence intensity of Cu-Fe/BC/Ag_3PO_4 was significantly reduced, indicating a lower band gap value that initiates electron movement from the valence to the conduction band. The photocatalytic degradation test revealed that the heterojunction BBP was capable of degrading phenol up to 100% within 18 min. ROS analysis indicated that h^+ and $\bullet O_2^-$ played a crucial role in the photodegradation of phenol. Furthermore, Density functional theory (DFT) analysis was carried out to comprehend the photodegradation mechanism, and the results indicated that electrons from Ag_3PO_4 migrated to the conduction band, then migrated to the valence band of $CuFe_2O_4$, while BC acted as an electron transport medium that inhibited electron hole pair recombination. In another study, Kumar and

colleagues developed a $C_3N_4/Bi_2O_2CO_3/CoFe_2O_4$ nano-assembled photocatalyst utilizing BC as a template for the growth of the catalyst for solar photodegradation of nitrophenol and paraquat (Kumar et al., 2018). The results indicated that BC facilitated electron transfer between the two different catalysts and inhibited recombination for a longer photoactivation. Photodegradation efficacy of 99.3% was achieved for nitrophenol and over 90% for paraquat. Electron spin resonance (EMS) and radical scavenging experiments confirmed that h^+ and $\bullet O_2^-$ played a significant role in the photodegradation of these phenolic compounds. The stability of the BBP was remarkable, as it exhibited a photoactivity efficiency of more than 98% after five reaction cycles, indicating the stability of BC as a template.

4.4 Dye

Researchers have taken a keen interest in dye wastewater generated by the textile industry. This industry, dating back to as early as 400 AD in India with the production of silk weaving, has witnessed a significant surge in recent decades. With the exponential growth of fast fashion, a category of inexpensive clothing produced rapidly by mass-market retailers in response to the latest trends, the consumption of such clothing has witnessed an unprecedented boom (Bailey et al., 2022). As a result, the increased production of clothing would lead to a direct increase in wastewater generated by the textile industry. With over 100,000 different dyes utilized in the dyeing process, even small amounts of dye present in water (as low as 10 ppm) can cause visible ecological problems. These issues include the blooming of algae, collapse of aquatic ecosystems, and contamination of large freshwater bodies (Behera et al., 2021). In recent years, researchers have turned to photocatalysis to degrade organic compounds and effectively remediate dye wastewater. Table 5 highlights some of the recent research employing BBP for the remediation of various frequently used dye molecules in the industry.

Table 5 Application of Biochar-Based Photocatalysts (BBP) for Dye Wastewater Remediation

BC composite	BC source	Surface area (m^2/g)	Light source	Pollutant	Major Reactive species	Removal % (loading)	Recyclability	Ref.
TiO_2-BC	chitosan	149.38	Xe Lamp 500W	Rhodamine B (RhB)	•OH and $•O_2^-$	98% (0.5)	90% (5^{th} cycle)	(Feng et al., 2022)
Fe_2O_3/TiO_2-BC	waste tea leaves	244.76	-	Methylene blue (MB)	•OH	99.7% (-)	66.1% (5^{th} cycle)	(Chen et al., 2020)
TiO_2-BC	microalgae	-	LED lamp 500W	MB	-	99% (2.0)	-	(Fazal et al., 2020)
Ag/TiO_2/BC	walnut shell	35.21	Mercury Lamp 500W	Methylene orange (MO)	h^+, $•O_2^-$ and •OH	97.48% (1.0)	96.10% (5^{th} cycle)	(Shan et al., 2020)
Fe_3O_4-BC	snake fruit peel	126.8	UV lamp 40W	RhB	•OH	99% (1.0)	99% (5^{th} cycle)	(Fatimah et al., 2022)
Bi_2WO_6/BC	orange peel	-	Xe lamp 45W	RhB	$•O_2^-$	94.9% (0.1)	91% (5^{th} cycle)	(Wu et al., 2022)
NiFe-LDH/BC	bamboo	23.29	Xe Lamp 300W	Reactive Red (RR120)	h^+ and •OH	88.5% (0.25)	-	(Luo et al., 2023)
Cu_2O-BC	wood powder	30.34	Simulated visible light	MO	$•O_2^-$	94.5% (1.0)	80% (5^{th} cycle)	(zhang et al., 2023)
BC-ZnO	maize	-	Xe lamp 500W	Saf	$•O_2^-$	83.5% (0.5)	-	(Kamal et al., 2022)

Shan et al. successfully developed a composite of BBP with Ag and TiO_2 via mixing, calcination, and photodeposition to photodegrade MO (Shan et al., 2020). The use of walnut shell as the source of BC resulted in the formation of a porous structure, which was evident in the higher surface area values of $Ag/TiO_2/BC$ (55.231 m^2/g) compared to TiO_2 (30.074 m^2/g). The porous nature of BC allowed for growth of Ag and TiO_2 nanoparticles on the surface and pores of BC, with even dispersion of the catalyst throughout the porous structure of BC confirmed by TEX and EDX analysis. Furthermore, the introduction of BC and Ag led to a red shift in light absorbance, allowing the composite to absorb visible light for photoexcitation, as shown by the lower band gap value of the composite BBP compared to the pristine catalyst (Mallesham et al., 2020). When tested for photocatalytic activity using MO as the model pollutant, it was evident that the composite BBP's lower band gap, higher active sites, and better charge separation had a significant impact on its degradation efficiency. In fact, the BBP achieved 97.48% degradation of MO within an hour, while pristine TiO_2 only achieved about 60% degradation within the same reaction time. Trapping experiments showed that •OH was the major reactive species generated during the photocatalytic reaction pathways. The BBP was also found to be recyclable for up to 5 cycles without any loss in efficacy, thanks to its stable nature with the catalyst precipitated on the active sites of BC anchored well via the carboxyl groups, allowing better stability and a lower possibility of photocorrosion. To improve the recyclability of the photocatalyst, Fatimah et al. developed a magnetically separable BBP using an indigenous snake fruit peel as the source of BC for the photodegradation of RhB (Fatimah et al., 2022). XRD analysis confirmed the formation of γ-Fe_2O_3 on the surfaces and pores of the BC, making the BBP magnetic. Morphology analysis showed that the formation of a porous BC structure with a pore size range between 8 to 20 nm, while the analysis also suggested a particle size range of between 5 to 20 nm with lattice fringes of 0.26nm. Although the surface area of the modified BBP was smaller (126.8 m^2/g) compared to the surface area of the BC (141.2 m^2/g), the optical properties of the prepared BBP showed a shift in light absorption capacity, with higher intensity in yellow emission. This suggests that charge separation efficiency may be improved due to improved surface recombination centers. The photocatalytic degradation efficiency for RhB was recorded as 99% within 120 min of visible light activation. Additionally, the surface hydroxyl functional group from the BBP contributed to an increase in affinity between the BBP and the positively structured RhB, resulting in enhanced contact between the catalyst and pollutant for faster reaction rates. The catalyst demonstrated high stability, as evidenced by its ability to maintain a high level of photoactivity (more than 95%

dye degradation) even after 5 cycles. Furthermore, the BBP was magnetically recollected from the treated wastewater, allowing for facile recycling.

Wood powder, a major by-product of the timber industry, has been identified as a promising carbon source for the development of black carbon. Xhang et al. have demonstrated this potential by utilizing residual wood powder to fabricate a black carbon framework, which was then used as a template for the preparation of a porous spherical Cu_2O-based composite photocatalyst (Xhang et al., 2023). To increase the porosity of the black carbon, it was washed with an alkali solution to remove impurities after carbonisation. This resulted in black carbon with a surface area of 837.60 m^2/g, as confirmed by surface area analysis, compared to 492.20 m^2/g for untreated black carbon. TEM analysis revealed the growth of a highly ordered spherical structure with an average size of 201.7 nm, attributable to the template provided by the porous black carbon. Photocatalytic degradation experiments demonstrated that the Cu_2O-based composite photocatalyst was able to degrade up to 94.5% of MO within 140 min under visible light irradiation. Integration of the Cu_2O catalyst into the pores of BC reduced the band gap to 2.05eV, thereby reducing the energy required for photoactivation. Additionally, EIS analysis confirmed that the electron transfer rate from valence to conduction band was quicker and exhibited slower recombination rate. These physicochemical properties worked synergistically to enhance the photocatalytic activity of the composite photocatalyst. Moreover, the composite photocatalyst was found to be stable and reusable, as confirmed by recyclability tests, where it was able to maintain its efficacy for up to 5 cycles.

5.0 Key Points, Challenges and Future Perspective

Over the past 30 years, a significant amount of research has been conducted in the development of heterogeneous photocatalysts, with numerous research articles highlighting their potential for remediating a wide range of polluted water. The appeal of these catalysts lies in their ability to photodegrade various organic pollutants non-selectively, making them a one-size-fits-all treatment. The rapid development of BBP suggests that its performance is highly dependent on several factors, such as the catalyst's composition and structure, its interaction with the light source, and its physical and electrical properties (e.g., surface area, pore size, band gap, photoluminescence, etc.). While doping (the addition of a foreign atom into the photocatalyst) has been the most widely used technique to lower band gaps and impart sensitivity under visible light, there is much more effort required to enhance the design of photocatalysts which can

improve their efficacy favourably. In this review, it can be agreed upon that the use of BC, a material produced from various forms of biomass waste, has shown significant potential in enhancing the performance of traditional photocatalysts by providing notable improvements in their physicochemical properties and photocatalytic efficiency. BC can serve as a substrate, providing a large surface area and porous network to hold more catalyst, while participating in the photocatalytic mechanism of electron excitation, either by being an electron sink and/or inhibiting the recombination of electron-hole pairs. Some of the key components in ensuring that the impact of BC can be maximized when developing BBP are listed below:

- The pre-treatment of BC is a critical step in determining the physical properties when developing a BBP. Although not all research follows this protocol, the activation of BC using acid or alkali mediums plays a significant role in enhancing the surface area and porosity of the BC before being used as a substrate for the development of BBP. As BC is produced from waste materials, impurities and various heavy metals can be present in the final BC after pyrolysis. Thus, cleaning the BC can improve its physical properties. Studies that employ pre-treatment of BC often report surface areas of more than 200 m^2/g compared to untreated BC samples, effectively promoting the development of BBP with a larger catalyst loading.
- Post-treatment methods such as ball milling can aid in the development of more uniformly sized BBP. BC can be prepared in various forms and sizes due to the fibrous nature of the organic biomass used. The use of ball milling or sieving can result in evenly sized BC, which facilitates the development of BBP using different synthesis techniques. In larger scales, the uniform size of BBP can play a critical role in the hydrodynamics of photoreactors that utilize such heterogeneous photocatalysts in an aqueous system.

In general, the results compiled here suggest that the various BBP developed are remarkably effective in degrading various organic pollutants, often achieving a degradation efficiency of more than 95% under visible light irradiation. The use of BC in the development of BBP has been twofold, as it provides a suitable substrate for the development of the photocatalyst while enhancing the physicochemical properties of the developed BBP, ultimately leading to enhanced efficacy under visible light sources. These BBP have demonstrated effectiveness in the degradation of different organic pollutants, but mainly focus on three categories, namely pharmaceutical, phenolic, and dye molecules, all of which are among the emerging and established pollutants that threaten water security. While BBP has shown tremendous potential,

there are some significant gaps and limitations that need to be addressed if such a catalyst is to be employed to tackle real wastewater. Some of the challenges are as follows:

- The use of various synthesis techniques to develop BBP showcases the adaptability of BC to different reaction conditions due to its stability. While most research has focused on the physical properties, photocatalytic efficacy, and recyclability of BBP, there has been minimal investigation into the interaction between the catalyst and BC. A fundamental understanding of how the catalyst interacts with BC could shed more light on its long-term stability. Most research articles have only conducted recyclability tests up to five cycles, which may not be sufficient to prove the catalyst's reusability. However, for BBP to be a viable catalyst for larger scale operations, long-term stability tests will be required. Understanding the fundamentals of the composite catalyst can provide important insights for the development of more efficient and stable BBP in the future.
- While the successful application of BBP under laboratory conditions is noteworthy, it is imperative to conduct research on implementing the catalyst in a unified system to translate the technology into a real-world solution. Most research experiments use low concentrations of pollutants (less than 50 mg/L), while real-life pollutant streams can have concentrations of up to 2000 mg/L (Hussain et al., 2015). Although the mechanics and efficacy of BBP have been reported frequently in research articles, it is necessary to move forward by employing these BBP in real-time wastewaters to understand their limitations and evaluate the types of process parameters (e.g., pH of the solution, minimum concentration of catalyst, light source) of photoreactors required to maintain the efficacy of the catalyst on a larger scale. Real-time wastewaters exhibit various unfavourable characteristics, such as varying pH levels and higher turbidity, interaction among pollutants present in the wastewater which can impact the final efficacy of BBP employed.
- The abundance of BC as a raw material for the development of visible light photocatalyst is undeniable. The availability of black carbon (BC) and its low production cost (between $222 and $584 per ton) make it an attractive and economically sustainable substrate for developing efficient photocatalysts (Xiao et al., 2020). When discussing the market growth of BC in the global market, it can be observed that the Asia-Pacific BC market was valued at $148.9 million USD in 2022, with a compound annual growth rate (CAGR) of nearly 12% expected in the next 10 years. Since BC is

produced as a by-product during the generation of energy through gasification or pyrolysis of biomass, its value remains relatively low due to the lack of technology for its utilization. Therefore, it becomes economically feasible and attractive to develop technologies such as BBP to harness its abundant availability. However, the practical application of this material for the development of BBP necessitates careful consideration. While the transformation of waste into a valuable resource is possible, it is not as straightforward as portrayed in research articles. The cleaning and processing of BC before its use on a large scale for the development of BBP would require a significant investment of time and money. Since BC is a waste product, a technoeconomic and life cycle analysis can provide insights into the feasibility of integrating BC into the development of catalysts capable of treating various types of wastewaters. Such analysis can also assess the potential value addition of waste biomass in developing large-scale pilot plants utilizing BBP.

Water is an indispensable resource for all life. However, the discharge of different types of pollutants into water streams poses a serious threat to the environment and public health. Mismanagement of this resource can result in water scarcity worldwide. It is essential to take legislative measures to prevent the disposal of harmful waste into water streams, as well as continuously improve techniques for remediation of polluted water bodies. The development of effective photocatalysts is crucial in creating a sustainable form of treatment for polluted water. BBP have demonstrated excellent catalytic activity in the remediation of various types of pollutants, including dyes, phenolic compounds, and pharmaceutical compounds. However, further research is needed to enhance our understanding of these catalysts. One particular point of interest is the structure of BC and its role as an electron sink in BBP. Although BC is a carbonaceous material, it is not yet clear how it works as an electron sink. Additionally, the impact of the size of BC on the efficacy of BBP has not been extensively studied. While most work focuses on the surface area and porosity of the material, the size of the BC used may also significantly influence the final physical properties of the developed BBP, which can highly influence its characteristics and efficacy. An ideal catalyst for treating various forms of wastewater is expected to have low loading, high surface area, high stability, the generation of large quantities of ROS, and long-term efficiency. With continuous research and development, BBP has the potential to become an effective and sustainable solution for water remediation.

Although BBP has demonstrated sustainability and efficiency in the laboratory, its application in more robust and larger setups such as reactors, pilot plants, and industrial scale systems is

still limited. It is crucial to explore the potential of these catalysts in real-world settings and retrofit them into existing wastewater treatment plans to demonstrate their effectiveness. Scaling up such technologies and exposing them to more challenging conditions can provide valuable insights into the efficacy of BBP in the removal of pollutants. Higher concentrations of pollutants, mixtures of different pollutants within a waste stream, and the presence of impurities can all impact the performance of BBP. Therefore, research on these factors can provide a deeper understanding of the catalyst's efficacy and help in the design of reactors or pilots for different streams, ensuring that the catalyst remains in optimum condition for removal of pollutants.

6.0 Conclusion

The use of BC as both a substrate and dopant in developing BBP has offered great promise in enhancing pollutant remediation technologies. This review was able to collate all the latest literature on the different techniques used in synthesising BBP which are effective in remedying various POPs present in waterways these days. While previous reviews have taken a more holistic approach in evaluating BBP, this review provides a detailed emphasis on the influence of different synthesis techniques towards both the physico-chemical characteristics and its influence towards photocatalytically degrading various POPs. BBPs such as TiO_2-BC, Fe_2O_3/TiO_2-BC, and Ag_3PO_4/Fe_3O_4-BC were successfully synthesized using various agricultural and poultry wastes, including wheat straw, bagasse, and swine sludge. Different synthesis techniques have been explored, with sol-gel, co-precipitation, hydrothermal synthesis, hydrolysis, and self-assembly being the most popular techniques. It has been discovered that post-treatment techniques, such as acid and alkali treatment, can help exfoliate BC, leading to enhanced porosity and surface area, which are crucial for developing efficient photocatalysts. These facile synthesis techniques have allowed researchers to develop various BBPs, which have consistently shown lower band gaps, improved charge separation, lower recombination rates, and enhanced photodegradation efficiency. The use of BC as a substrate and dopant has led to increased active sites for photodegradation, while BC also acts as an electron sink, providing a longer pathway for electron transport and prolonging photoactivation. The prepared BBPs have also demonstrated enhanced photoactivity by incorporating BC into their matrix, achieving highly efficient photodegradation of more than 95% for various pollutants, including pharmaceuticals, dyes, and phenolic compounds, such as triclosan, ciprofloxacin, bisphenol-a, nitrophenols, MB, and RhB, among others. This review also highlights the enormous potential exhibited by BBPs in water remediation processes in

small and larger industrial scales. However, more research is needed to confirm the feasibility of scaling up. Herein, emphasis on technical viability, long-term stability, and incorporation of BBPs into current wastewater remediation technologies is needed to shed more information on its potential. The current state in literature clearly highlights that the implementation of BBPs into current wastewater technologies to remediate wastewater is in its infancy, more emphasis is required in scaling up both the synthesis of efficient BBPs as well as implementing them in remedying real time wastewaters.

Acknowledgement: The authors would like to acknowledge the funding support provided by The Royal Society (IEC\NSFC\201014) in the United Kingdom, and the European Union's Horizon 2020 Research and Innovation Program under Grant Agreement N° 862330 (INNOMEM).

References

Al-Tohamy, R, Ali, S.S., Li, F., Okasha, K.M., Mahmoud, Y.A.-G., Elsamahy, T., Jiao, H., Fu, Y., Sun, J. A critical review on the treatment of dye-containing wastewater: Ecotoxicological and health concerns of textile dyes and possible remediation approaches for environmental safety. Ecotoxicol. Environ. Saf. 231, 113160. https://doi.org/10.1016/j.ecoenv.2021.113160

Amir, M., Fazal, T., Iqbal, J., Din, A.A., Ahmed, A., Ali, A., Razzaq, A., Ali, Z., Rehman, M.S.U., Park, Y.-K., 2022. Integrated adsorptive and photocatalytic degradation of pharmaceutical micropollutant, ciprofloxacin employing biochar-ZnO composite photocatalysts. J. Ind. Eng. Chem. 115, 171–182. https://doi.org/https://doi.org/10.1016/j.jiec.2022.07.050

Azalok, K.A., Oladipo, A.A., Gazi, M., 2021. UV-light-induced photocatalytic performance of reusable MnFe-LDO–biochar for tetracycline removal in water. J. Photochem. Photobiol. A Chem. 405, 112976. https://doi.org/https://doi.org/10.1016/j.jphotochem.2020.112976

Bailey, K., Basu, A., Sharma, S., 2022. The Environmental Impacts of Fast Fashion on Water Quality: A Systematic Review. Water. https://doi.org/10.3390/w14071073

Behera, M., Nayak, J., Banerjee, S., Chakrabortty, S., Tripathy, S.K., 2021. A review on the

treatment of textile industry waste effluents towards the development of efficient mitigation strategy: An integrated system design approach. J. Environ. Chem. Eng. 9, 105277. https://doi.org/https://doi.org/10.1016/j.jece.2021.105277

Cai, X., Li, J., Liu, Y., Yan, Z., Tan, X., Liu, S., Zeng, G., Gu, Y., Hu, X., Jiang, L., 2018. Titanium dioxide-coated biochar composites as adsorptive and photocatalytic degradation materials for the removal of aqueous organic pollutants. J. Chem. Technol. Biotechnol. 93, 783–791. https://doi.org/https://doi.org/10.1002/jctb.5428

Cao, T., Zhou, D., Wang, X., Cui, C., 2022. Photocatalytic degradation of bisphenol A over Co-BiOCl/biochar hybrid catalysts: Properties, efficiency and mechanism. J. Mol. Liq. 362, 119622. https://doi.org/https://doi.org/10.1016/j.molliq.2022.119622

Chatterjee, R., Sajjadi, B., Chen, W., Mattern, D.L., Hammer, N., 2020. Effect of Pyrolysis Temperature on PhysicoChemical Properties and Acoustic-Based Amination of Biochar for Efficient CO_2 Adsorption. Front. Energy Res. 8, 1–18. https://doi.org/10.3389/fenrg.2020.00085

Chen, Mingxin, Bao, C., Hu, D., Jin, X., Huang, Q., 2019. Facile and low-cost fabrication of ZnO / biochar nanocomposites from jute fibers for efficient and stable photodegradation of methylene blue dye. J. Anal. Appl. Pyrolysis 139, 319–332. https://doi.org/10.1016/j.jaap.2019.03.009

Chen, Minxing, Dai, Y., Guo, J., Yang, H., Liu, D., Zhai, Y., 2019. Solvothermal synthesis of biochar@$ZnFe_2O_4$/BiOBr Z-scheme heterojunction for efficient photocatalytic ciprofloxacin degradation under visible light. Appl. Surf. Sci. 493, 1361–1367. https://doi.org/https://doi.org/10.1016/j.apsusc.2019.04.160

Chen, R., Fan, F., Li, C., 2022. Unraveling Charge-Separation Mechanisms in Photocatalyst Particles by Spatially Resolved Surface Photovoltage Techniques. Angew. Chemie - Int. Ed. 61. https://doi.org/10.1002/anie.202117567

Chen, X.-L., Li, F., Chen, H., Wang, H., Li, G., 2020. Fe_2O_3/TiO_2 functionalized biochar as a heterogeneous catalyst for dyes degradation in water under Fenton processes. J. Environ. Chem. Eng. 8, 103905. https://doi.org/https://doi.org/10.1016/j.jece.2020.103905

Chen, X., Zhang, M., Qin, H., Zhou, J., Shen, Q., Wang, K., Chen, W., Liu, M., Li, N., 2022. Synergy effect between adsorption and heterogeneous photo-Fenton-like catalysis on

$LaFeO_3$/lignin-biochar composites for high efficiency degradation of ofloxacin under visible light. Sep. Purif. Technol. 280, 119751. https://doi.org/https://doi.org/10.1016/j.seppur.2021.119751

Chen, Z., He, Z., Zhou, M., Xie, M., He, T., Zhao, Y., Chen, X., Wu, Y., Xu, Z., 2021. In-situ synthesis of biochar modified $PbMoO_4$: An efficient visible light-driven photocatalyst for tetracycline removal. Chemosphere 284, 131260. https://doi.org/https://doi.org/10.1016/j.chemosphere.2021.131260

Cufe, O., Liu, Y., 2019. Insights into the interfacial carrier behaviour of copper ferrite ($CuFe_2O_4$) photoanodes for solar water oxidation. J. Mater. Chem. A 7, 1669–1677. https://doi.org/10.1039/c8ta11160j

Dharma, H.N.C., Jaafar, J., Widiastuti, N., Matsuyama, H., Rajabsadeh, S., Othman, M.H.D., Rahman, M.A., Jafri, N.N.M., Suhaimin, N.S., Nasir, A.M., Alias, N.H., 2022. A Review of Titanium Dioxide (TiO_2)-Based Photocatalyst for Oilfield-Produced Water Treatment. Membranes (Basel). 12. https://doi.org/10.3390/membranes12030345

Draper, K., Tomlinson, T., 2012. Poultry Litter Biochar – a US Perspective. Int. Biochar Initiat. 6.

Elgohary, E.A., Mohamed, Y.M.A., Nazer, H.A. El, Baaloudj, O., Alyami, M.S.S., Jery, A. El, Assadi, A.A., Amrane, A., 2021. A Review of the Use of Semiconductors as Catalysts in the Photocatalytic Inactivation of Microorganisms. Catalysts 1–15.

Eniola, J.O., Kumar, R., Barakat, M.A., Rashid, J., 2022. A review on conventional and advanced hybrid technologies for pharmaceutical wastewater treatment. J. Clean. Prod. 356, 131826. https://doi.org/https://doi.org/10.1016/j.jclepro.2022.131826

Fatimah, I., Purwiandono, G., Sahroni, I., Wijayana, A., Faraswati, M., Dwi Putri, A., Oh, W.-C., Doong, R., 2022. Magnetically-separable photocatalyst of magnetic biochar from snake fruit peel for rhodamine B photooxidation. Environ. Nanotechnology, Monit. Manag. 17, 100669. https://doi.org/https://doi.org/10.1016/j.enmm.2022.100669

Fazal, T., Razzaq, A., Javed, F., Hafeez, A., Rashid, N., Amjad, U.S., Ur Rehman, M.S., Faisal, A., Rehman, F., 2020. Integrating adsorption and photocatalysis: A cost effective strategy for textile wastewater treatment using hybrid biochar-TiO_2 composite. J. Hazard. Mater. 390, 121623. https://doi.org/https://doi.org/10.1016/j.jhazmat.2019.121623

Feng, X., Li, X., Su, B., Ma, J., 2022. Solid-phase fabrication of TiO_2/Chitosan-biochar composites with superior UV–vis light driven photocatalytic degradation performance. Colloids Surfaces A Physicochem. Eng. Asp. 648, 129114. https://doi.org/https://doi.org/10.1016/j.colsurfa.2022.129114

Fito, J., Kefeni, K.K., Nkambule, T.T.I., 2022. The potential of biochar-photocatalytic nanocomposites for removal of organic micropollutants from wastewater. Sci. Total Environ. 829, 154648. https://doi.org/https://doi.org/10.1016/j.scitotenv.2022.154648

Gao, W., Lu, J., Zhang, S., Zhang, X., Wang, Z., Qin, W., Wang, J., Zhou, W., Liu, H., Sang, Y., 2019. Suppressing Photoinduced Charge Recombination via the Lorentz Force in a Photocatalytic System. Adv. Sci. 6, 1901244. https://doi.org/https://doi.org/10.1002/advs.201901244

Gholami, P., Khataee, A., Soltani, R.D.C., Dinpazhoh, L., Bhatnagar, A., 2020. Photocatalytic degradation of gemifloxacin antibiotic using Zn-Co-LDH@biochar nanocomposite. J. Hazard. Mater. 382, 121070. https://doi.org/https://doi.org/10.1016/j.jhazmat.2019.121070

Gonçalves, N.P.F., Lourenço, M.A.O., Baleuri, S.R., Bianco, S., Jagdale, P., Calza, P., 2022. Biochar waste-based ZnO materials as highly efficient photocatalysts for water treatment. J. Environ. Chem. Eng. 10, 107256. https://doi.org/https://doi.org/10.1016/j.jece.2022.107256

Hama Aziz, K.H., Mustafa, F.S., Omer, K.M., Hama, S., Hamarawf, R.F., Rahman, K.O., 2023. Heavy metal pollution in the aquatic environment: efficient and low-cost removal approaches to eliminate their toxicity: a review. RSC Adv. 13, 17595–17610. https://doi.org/10.1039/d3ra00723e

Hossain, N., Nizamuddin, S., Griffin, G., Selvakannan, P., Mubarak, N.M., Mahlia, T.M.I., 2020. Synthesis and characterization of rice husk biochar via hydrothermal carbonization for wastewater treatment and biofuel production. Sci. Rep. 10, 1–15. https://doi.org/10.1038/s41598-020-75936-3

Hosseini-Monfared, H., Mohammadi, Y., Montazeri, R., 2021. Effect of biochar on the photocatalytic activity of nitrogen-doped titanium dioxide nanocomposite in the removal of aqueous organic pollutants under visible light. Nanochemres.Org 6, 79–93. https://doi.org/10.22036/ncr.2021.01.008

Hu, H., Lin, Y., Hu, Y.H., 2020. Core-shell structured TiO_2 as highly efficient visible light photocatalyst for dye degradation. Catal. Today 341, 90–95. https://doi.org/https://doi.org/10.1016/j.cattod.2019.01.077

Hu, Xi, Hu, Xinjiang, Tang, C., Wen, S., Wu, X., Long, J., Yang, X., Wang, H., Zhou, L., 2017. Mechanisms underlying degradation pathways of microcystin-LR with doped TiO_2 photocatalysis. Chem. Eng. J. 330, 355–371. https://doi.org/https://doi.org/10.1016/j.cej.2017.07.161

Hussain, A., Dubey, S.K., Kumar, V., 2015. Kinetic study for aerobic treatment of phenolic wastewater. Water Resour. Ind. 11, 81–90. https://doi.org/https://doi.org/10.1016/j.wri.2015.05.002

Kamal, A., Saleem, M.H., Alshaya, H., Okla, M.K., Chaudhary, H.J., Munis, M.F.H., 2022. Ball-milled synthesis of maize biochar-ZnO nanocomposite (MB-ZnO) and estimation of its photocatalytic ability against different organic and inorganic pollutants. J. Saudi Chem. Soc. 26, 101445. https://doi.org/https://doi.org/10.1016/j.jscs.2022.101445

Kanani, F., Heidari, M.D., Gilroyed, B.H., Pelletier, N., 2020. Waste valorization technology options for the egg and broiler industries: A review and recommendations. J. Clean. Prod. 262, 121129. https://doi.org/https://doi.org/10.1016/j.jclepro.2020.121129

Ke, J., Ge, Y., Yang, Q., Liu, Y., Show, P.-L., Guo, R., Chen, J., 2022. Degradation of sulfamethazine using sludge-derived photocatalysts from dyeing industry and livestock farm: preparation and mechanism. J. Hazard. Mater. 440, 129837. https://doi.org/https://doi.org/10.1016/j.jhazmat.2022.129837

Khairy, M., Ibrahim, M.A.M., Sekiguchi, S.O.H., 2023. The influence of torrefaction on the biochar characteristics produced from sesame stalks and bean husk. Biomass Convers. Biorefinery. https://doi.org/10.1007/s13399-023-03822-9

Kim, D., Yoshikawa, K., Park, K.Y., 2015. Characteristics of biochar obtained by hydrothermal carbonization of cellulose for renewable energy. Energies 8, 14040–14048. https://doi.org/10.3390/en81212412

Kruusenberg, I., Stojanovska, E., Pampal, E.S., Kilic, A., Wu, T., Li, X., 2021. A Review On The Comparison Between Slow Pyrolysis And Fast Pyrolysis On The Quality Of Lignocellulosic And Lignin- Based Biochar. IOP Conf. Ser. Mater. Sci. Eng. 263 1051.

https://doi.org/10.1088/1757-899X/1051/1/012075

Kumar, Amit, Kumar, Ajay, Sharma, G., Al-Muhtaseb, A.H., Naushad, M., Ghfar, A.A., Guo, C., Stadler, F.J., 2018. Biochar-templated g-C_3N_4/$Bi_2O_2CO_3$/$CoFe_2O_4$ nano-assembly for visible and solar assisted photo-degradation of paraquat, nitrophenol reduction and CO2 conversion. Chem. Eng. J. 339, 393–410. https://doi.org/https://doi.org/10.1016/j.cej.2018.01.105

Kumar Ray, S., Anil Kumar Reddy, P., Yoon, S., Shin, J., Chon, K., Bae, S., 2023. A magnetically separable α-$NiMoO_4$/$ZnFe_2O_4$/coffee biochar heterojunction photocatalyst for efficient ketoprofen degradation. Chem. Eng. J. 452, 139546. https://doi.org/https://doi.org/10.1016/j.cej.2022.139546

Le, P.T., Le, D.N., Nguyen, T.H., Bui, H.T., Pham, L.A., Nguyen, L.L., Nguyen, Q.S., Nguyen, T.P., Dang, T.H., Duong, T.T., Herrmann, M., Ouillon, S., Le, T.P., Vo, D.L., Mai, H., Dinh, T.M., 2021. On the Degradation of Glyphosate by Photocatalysis Using TiO_2/Biochar Composite Obtained from the Pyrolysis of Rice Husk. Water. https://doi.org/10.3390/w13233326

Lee, J.E., Park, Y.K., 2020. Applications of modified biochar-based materials for the removal of environment pollutants: A mini review. Sustain. 12. https://doi.org/10.3390/su12156112

Leichtweis, J., Silvestri, S., Welter, N., Vieira, Y., Zaragoza-Sánchez, P.I., Chávez-Mejía, A.C., Carissimi, E., 2021. Wastewater containing emerging contaminants treated by residues from the brewing industry based on biochar as a new $CuFe_2O_4$ / biochar photocatalyst. Process Saf. Environ. Prot. 150, 497–509. https://doi.org/https://doi.org/10.1016/j.psep.2021.04.041

Li, D., Song, H., Meng, X., Shen, T., Sun, J., Han, W., Wang, X., 2020. Effects of Particle Size on the Structure and Photocatalytic Performance by Alkali-Treated TiO_2. Nanomater. (Basel, Switzerland) 10. https://doi.org/10.3390/nano10030546

Li, H., Hu, J., Zhou, X., Li, X., Wang, X., 2018. An investigation of the biochar-based visible-light photocatalyst via a self-assembly strategy. J. Environ. Manage. 217, 175–182. https://doi.org/https://doi.org/10.1016/j.jenvman.2018.03.083

Li, M., Li, P., Zhang, L., Chen, M., Tang, J., Qin, C., Ling Jie Lee, S., Lin, S., 2022. Facile

fabrication of ZnO decorated ZnFe-layered double hydroxides @ biochar nanocomposites for synergistic photodegradation of tetracycline under visible light. Chem. Eng. J. 434, 134772. https://doi.org/https://doi.org/10.1016/j.cej.2022.134772

Li, X., Fang, G., Qian, X., Tian, Q., 2022. Z-scheme heterojunction of low conduction band potential MnO_2 and biochar-based g-C_3N_4 for efficient formaldehyde degradation. Chem. Eng. J. 428, 131052. https://doi.org/https://doi.org/10.1016/j.cej.2021.131052

Liang, H., Zi, H., Huang, H., Jia, W., 2022. Comparative study of Ti - alkaline biochar and Ti - acidic biochar photo catalysts for degradation of methyl orange. Clean Technol. Environ. Policy. https://doi.org/10.1007/s10098-022-02426-7

Lin, M., Li, F., Cheng, W., Rong, X., Wang, W., 2022. Facile preparation of a novel modified biochar-based supramolecular self-assembled g-C_3N_4 for enhanced visible light photocatalytic degradation of phenanthrene. Chemosphere 288, 132620. https://doi.org/https://doi.org/10.1016/j.chemosphere.2021.132620

Liu, C., Wang, W., Wu, R., Liu, Y., Lin, X., Kan, H., Zheng, Y., 2020. Preparation of Acid- and Alkali-Modified Biochar for Removal of Methylene Blue Pigment. ACS Omega 5, 30906–30922. https://doi.org/10.1021/acsomega.0c03688

Liu, X., Zhou, J., Wang, G., Liu, D., Liu, S., 2022. Construction of Cu-Fe bimetallic oxide/biochar/Ag_3PO_4 heterojunction for improving photocorrosion resistance and photocatalytic performance achieves efficient removal of phenol. Appl. Surf. Sci. 592, 153307. https://doi.org/https://doi.org/10.1016/j.apsusc.2022.153307

Luo, H., Yu, S., Zhong, M., Han, Y., Su, B., Lei, Z., 2022. Waste biomass-assisted synthesis of TiO_2 and N/O-contained graphene-like biochar composites for enhanced adsorptive and photocatalytic performances. J. Alloys Compd. 899, 163287. https://doi.org/https://doi.org/10.1016/j.jallcom.2021.163287

Luo, Y., Wang, Y., Hua, F., Xue, M., Xie, X., Xie, Y., Yu, S., Zhang, L., Yin, Z., Xie, C., Hong, Z., 2023. Adsorption and photodegradation of reactive red 120 with nickel-iron-layered double hydroxide/biochar composites. J. Hazard. Mater. 443, 130300. https://doi.org/https://doi.org/10.1016/j.jhazmat.2022.130300

Ma, Y., Zhang, T., Zhu, P., Cai, H., Jin, Y., Gao, K., Li, J., 2022. Fabrication of Ag_3PO_4/polyaniline-activated biochar photocatalyst for efficient triclosan degradation

process and toxicity assessment. Sci. Total Environ. 821, 153453. https://doi.org/https://doi.org/10.1016/j.scitotenv.2022.153453

Mallesham, B., Roy, S., Bose, S., Nair, A.N., Sreenivasan, S., Shutthanandan, V., Ramana, C. V, 2020. Crystal Chemistry, Band-Gap Red Shift, and Electrocatalytic Activity of Iron-Doped Gallium Oxide Ceramics. ACS Omega 5, 104–112. https://doi.org/10.1021/acsomega.9b01604

Mankomal, Kaur, H., 2022. Synergistic effect of biochar impregnated with ZnO nano-flowers for effective removal of organic pollutants from wastewater. Appl. Surf. Sci. Adv. 12, 100339. https://doi.org/https://doi.org/10.1016/j.apsadv.2022.100339

Mian, M.M. and Liu, G. Recent progress in biochar-supported photocatalysts: synthesis, role of biochar, and applications. RSC Adv., 2018, 8, 14237-14248. DOI: 10.1039/C8RA02258E

Mustafa, F.S., Hama Aziz, K.H., 2023. Heterogeneous catalytic activation of persulfate for the removal of rhodamine B and diclofenac pollutants from water using iron-impregnated biochar derived from the waste of black seed pomace. Process Saf. Environ. Prot. 170, 436–448. https://doi.org/https://doi.org/10.1016/j.psep.2022.12.030

Muvhiiwa, R., Kuvarega, A., Llana, E.M., Muleja, A., 2019. Study of biochar from pyrolysis and gasification of wood pellets in a nitrogen plasma reactor for design of biomass processes. J. Environ. Chem. Eng. 7, 103391. https://doi.org/https://doi.org/10.1016/j.jece.2019.103391

Nair, R. V., Gummaluri, V.S., Matham, M.V., Vijayan, C., 2022. A review on optical bandgap engineering in TiO_2 nanostructures via doping and intrinsic vacancy modulation towards visible light applications. J. Phys. D. Appl. Phys. 55. https://doi.org/10.1088/1361-6463/ac6135

Pan, X., Gu, Z., Chen, W., Li, Q., 2021. Preparation of biochar and biochar composites and their application in a Fenton-like process for wastewater decontamination: A review. Sci. Total Environ. 754, 142104. https://doi.org/https://doi.org/10.1016/j.scitotenv.2020.142104

Peng, H., Wang, L., Zheng, X., 2023. Efficient adsorption-photodegradation activity of MoS_2 coupling with S,N-codoped porous biochar derived from chitosan. J. Water Process Eng.

51, 103426. https://doi.org/https://doi.org/10.1016/j.jwpe.2022.103426

Qadir, M., Drechsel, P., Jiménez Cisneros, B., Kim, Y., Pramanik, A., Mehta, P., Olaniyan, O., 2020. Global and regional potential of wastewater as a water, nutrient and energy source. Nat. Resour. Forum 44, 40–51. https://doi.org/https://doi.org/10.1111/1477-8947.12187

Qian, R., Zong, H., Schneider, J., Zhou, G., Zhao, T., Li, Y., Yang, J., Bahnemann, D.W., Pan, J.H., 2019. Charge carrier trapping, recombination and transfer during TiO_2 photocatalysis: An overview. Catal. Today 335, 78–90. https://doi.org/https://doi.org/10.1016/j.cattod.2018.10.053

Qu, K., Huang, L., Hu, S., Liu, C., Yang, Q., Liu, L., Li, K., Zhao, Z., Wang, Z., 2023. TiO_2 supported on rice straw biochar as an adsorptive and photocatalytic composite for the efficient removal of ciprofloxacin in aqueous matrices. J. Environ. Chem. Eng. 11, 109430. https://doi.org/https://doi.org/10.1016/j.jece.2023.109430

Reguyal, F., Sarmah, A.K., Gao, W., 2017. Synthesis of magnetic biochar from pine sawdust via oxidative hydrolysis of FeCl2 for the removal sulfamethoxazole from aqueous solution. J. Hazard. Mater. 321, 868–878. https://doi.org/10.1016/j.jhazmat.2016.10.006

Rosman, N., Salleh, W.N.W., Mohamed, M.A., Jaafar, J., Ismail, A.F., Harun, Z., 2018. Hybrid membrane filtration-advanced oxidation processes for removal of pharmaceutical residue. J. Colloid Interface Sci. 532, 236–260. https://doi.org/10.1016/j.jcis.2018.07.118

Samy, M., Gar Alalm, M., Khalil, M.N., Ezeldean, E., El-Dissouky, A., Nasr, M., Tawfik, A., 2023. Treatment of hazardous landfill leachate containing 1,4 dioxane by biochar-based photocatalysts in a solar photo-oxidation reactor. J. Environ. Manage. 332, 117402. https://doi.org/https://doi.org/10.1016/j.jenvman.2023.117402

Sathishkumar, K., Li, Y., Sanganyado, E., 2020. Electrochemical behavior of biochar and its effects on microbial nitrate reduction: Role of extracellular polymeric substances in extracellular electron transfer. Chem. Eng. J. 395, 125077. https://doi.org/https://doi.org/10.1016/j.cej.2020.125077

Shaaban, M., Van Zwieten, L., Bashir, S., Younas, A., Núñez-Delgado, A., Chhajro, M.A., Kubar, K.A., Ali, U., Rana, M.S., Mehmood, M.A., Hu, R., 2018. A concise review of biochar application to agricultural soils to improve soil conditions and fight pollution. J. Environ. Manage. 228, 429–440.

https://doi.org/https://doi.org/10.1016/j.jenvman.2018.09.006

Shan, R., Lu, L., Gu, J., Zhang, Y., Yuan, H., Chen, Y., Luo, B., 2020. Photocatalytic degradation of methyl orange by Ag/TiO_2/biochar composite catalysts in aqueous solutions. Mater. Sci. Semicond. Process. 114, 105088. https://doi.org/https://doi.org/10.1016/j.mssp.2020.105088

Shishido, T., Teramura, K., Tanaka, T., 2011. A unique photo-activation mechanism by "in situ doping" for photo-assisted selective NO reduction with ammonia over TiO_2 and photooxidation of alcohols over Nb2O5. Catal. Sci. Technol. 1, 541–551. https://doi.org/10.1039/C1CY00104C

Song, J., Wang, Y., Lv, Z., Li, Y., Cao, X., Cheng, W., 2023. Degradation of nonylphenol ethoxylate 10 in biochar-$CoFe_2O_4$/peroxymonosulfate system: Transformation products identification, catalysis mechanism and influencing factors. J. Environ. Chem. Eng. 11, 109241. https://doi.org/https://doi.org/10.1016/j.jece.2022.109241

Sutar, S., Otari, S., Jadhav, J., 2022. Biochar based photocatalyst for degradation of organic aqueous waste: A review. Chemosphere 287, 132200. https://doi.org/https://doi.org/10.1016/j.chemosphere.2021.132200

Talukdar, K., Jun, B.-M., Yoon, Y., Kim, Y., Fayyaz, A., Park, C.M., 2020. Novel Z-scheme Ag_3PO_4/Fe_3O_4-activated biochar photocatalyst with enhanced visible-light catalytic performance toward degradation of bisphenol A. J. Hazard. Mater. 398, 123025. https://doi.org/https://doi.org/10.1016/j.jhazmat.2020.123025

Tariq, M., Ali Baig, S., Shams, D.F., Hussain, S., Hussain, R., Qadir, A., Maryam, H.S., Khan, Z.U., Sattar, S., Xu, X., 2022. Dye Wastewater Treatment Using Wheat Straw Biochar in Gadoon Industrial Areas of Swabi, Pakistan. Water Conserv. Sci. Eng. 7, 315–326. https://doi.org/10.1007/s41101-022-00144-1

Tomczyk, A., 2020. Biochar physicochemical properties : pyrolysis temperature and feedstock kind effects. Rev. Environ. Sci. Bio/Technology 19, 191–215. https://doi.org/10.1007/s11157-020-09523-3

Wang, H., Guo, W., Si, Q., Liu, B., Zhao, Q., Luo, H., Ren, N., 2021. Multipath elimination of bisphenol A over bifunctional polymeric carbon nitride/biochar hybrids in the presence of persulfate and visible light. J. Hazard. Mater. 417, 126008.

https://doi.org/https://doi.org/10.1016/j.jhazmat.2021.126008

Wang, T., Cai, J., Zheng, J., Fang, K., Hussain, I., Husein, D.Z., 2022. Facile synthesis of activated biochar/$BiVO_4$ heterojunction photocatalyst to enhance visible light efficient degradation for dye and antibiotics: applications and mechanisms. J. Mater. Res. Technol. 19, 5017–5036. https://doi.org/https://doi.org/10.1016/j.jmrt.2022.06.177

Wang, W., Zhang, J., Chen, T., Sun, J., Ma, X., Wang, Y., Wang, J., Xie, Z., 2020. Preparation of TiO_2-modified Biochar and its Characteristics of Photo-catalysis Degradation for Enrofloxacin. Sci. Rep. 10, 6588. https://doi.org/10.1038/s41598-020-62791-5

Wang, Y., Yin, R., Liu, R., 2014. Characterization of biochar from fast pyrolysis and its effect on chemical properties of the tea garden soil. J. Anal. Appl. Pyrolysis 110, 375–381. https://doi.org/https://doi.org/10.1016/j.jaap.2014.10.006

Water Scarcity | Threats | WWF [WWW Document], n.d. URL https://www.worldwildlife.org/threats/water-scarcity (accessed 9.29.22).

Wear, S.L., Acuña, V., McDonald, R., Font, C., 2021. Sewage pollution, declining ecosystem health, and cross-sector collaboration. Biol. Conserv. 255, 109010. https://doi.org/https://doi.org/10.1016/j.biocon.2021.109010

Wei, X., Xu, X., Yang, X., Liu, Z., Naraginti, S., Sen, L., Weidi, S., Buwei, L., 2022. Novel assembly of $BiVO_4$@N-Biochar nanocomposite for efficient detoxification of triclosan. Chemosphere 298, 134292. https://doi.org/https://doi.org/10.1016/j.chemosphere.2022.134292

Wei, X., Yu, F., Ji, J., Cai, Y., Zou, W., Zheng, Y., Huang, J., Zhang, Y., Yang, Y., Naushad, M., Gao, B., Dong, L., 2021. Porous biochar supported Ag_3PO_4 photocatalyst for "two-in-one" synergistic adsorptive-photocatalytic removal of methylene blue under visible light irradiation. J. Environ. Chem. Eng. 9, 106753. https://doi.org/10.1016/j.jece.2021.106753

Welter, N., Leichtweis, J., Silvestri, S., Sánchez, P.I.Z., Mejía, A.C.C., Carissimi, E., 2022. Preparation of a new green composite based on chitin biochar and $ZnFe_2O_4$ for photo-Fenton degradation of Rhodamine B. J. Alloys Compd. 901, 163758. https://doi.org/https://doi.org/10.1016/j.jallcom.2022.163758

Wu, G., Liu, Q., Wang, J., Zhang, Y., Yu, C., Bian, H., Hegazy, M., Han, J., Xing, W., 2022.

Facile fabrication of Bi_2WO_6/biochar composites with enhanced charge carrier separation for photodecomposition of dyes. Colloids Surfaces A Physicochem. Eng. Asp. 634, 127945. https://doi.org/https://doi.org/10.1016/j.colsurfa.2021.127945

Xiao, L., Feng, L., Yuan, G., Wei, J., 2020. Low-cost field production of biochars and their properties. Environ. Geochem. Health 42, 1569–1578. https://doi.org/10.1007/s10653-019-00458-5

Xie, X., Li, S., Qi, K., Wang, Z., 2021. Photoinduced synthesis of green photocatalyst Fe_3O_4/BiOBr/CQDs derived from corncob biomass for carbamazepine degradation: The role of selectively more CQDs decoration and Z-scheme structure. Chem. Eng. J. 420, 129705. https://doi.org/https://doi.org/10.1016/j.cej.2021.129705

Xie, Y., Liu, A., Bandala, E.R., Goonetilleke, A., 2022. TiO_2-biochar composites as alternative photocatalyst for stormwater disinfection. J. Water Process Eng. 48, 102913. https://doi.org/https://doi.org/10.1016/j.jwpe.2022.102913

Xin, D., Barkley, T., Chiu, P.C., 2020. Visualizing electron storage capacity distribution in biochar through silver tagging. Chemosphere 248, 125952. https://doi.org/https://doi.org/10.1016/j.chemosphere.2020.125952

Xin, D., Saha, N., Reza, M.T., Hudson, J., Chiu, P.C., 2021. Pyrolysis Creates Electron Storage Capacity of Black Carbon (Biochar) from Lignocellulosic Biomass. ACS Sustain. Chem. Eng. 9, 6821–6831. https://doi.org/10.1021/acssuschemeng.1c01251

Yaashikaa, P.R., Kumar, P.S., Varjani, S., Saravanan, A., 2020. A critical review on the biochar production techniques, characterization, stability and applications for circular bioeconomy. Biotechnol. Reports 28, e00570. https://doi.org/https://doi.org/10.1016/j.btre.2020.e00570

Youssef, Z., Colombeau, L., Yesmurzayeva, N., Baros, F., Vanderesse, R., Hamieh, T., Toufaily, J., Frochot, C., Roques-Carmes, T., 2018. Dye-sensitized nanoparticles for heterogeneous photocatalysis: Cases studies with TiO_2, ZnO, fullerene and graphene for water purification. Dye. Pigment. 159, 49–71. https://doi.org/10.1016/j.dyepig.2018.06.002

Yuan, J., Wen, Y., Dionysiou, D.D., Sharma, V.K., Ma, X., 2022. Biochar as a novel carbon-negative electron source and mediator: electron exchange capacity (EEC) and

environmentally persistent free radicals (EPFRs): a review. Chem. Eng. J. 429, 132313. https://doi.org/https://doi.org/10.1016/j.cej.2021.132313

Zhai, Y., Dai, Y., Guo, J., Zhou, L., Chen, M., Yang, H., Peng, L., 2020. Novel biochar@$CoFe_2O_4$/Ag_3PO_4 photocatalysts for highly efficient degradation of bisphenol a under visible-light irradiation. J. Colloid Interface Sci. 560, 111–121. https://doi.org/https://doi.org/10.1016/j.jcis.2019.08.065

Zhang, H., Wang, Z., Li, R., Guo, J., Li, Y., Zhu, J., Xie, X., 2017. TiO_2 supported on reed straw biochar as an adsorptive and photocatalytic composite for the efficient degradation of sulfamethoxazole in aqueous matrices. Chemosphere 185, 351–360. https://doi.org/https://doi.org/10.1016/j.chemosphere.2017.07.025

Zhang, X., Guo, M., Liu, S., Xiang, H., Guo, X., Yang, Y., 2021. Performance and mechanism of biochar-coupled $BiVO_4$ photocatalyst on the degradation of sulfanilamide. J. Clean. Prod. 325, 129349. https://doi.org/https://doi.org/10.1016/j.jclepro.2021.129349

Zhang, Y., Fan, R., Zhang, Q., Chen, Y., Shari, O., Leszczynska, D., 2019. Synthesis of CaWO 4 -biochar nanocomposites for organic dye removal. Mater. Res. Bull. 110, 169–173.

zhang, Y., Li, X., Chen, J., Wang, Y., Cheng, Z., Chen, X., Gao, X., Guo, M., 2023. Porous spherical Cu_2O supported by wood-based biochar skeleton for the adsorption-photocatalytic degradation of methyl orange. Appl. Surf. Sci. 611, 155744. https://doi.org/https://doi.org/10.1016/j.apsusc.2022.155744

Zheng, M.-W., Yang, S.-J., Pu, Y.-C., Liu, S.-H., 2022. Mechanisms of biochar enhanced Cu_2O photocatalysts in the visible-light photodegradation of sulfamethoxazole. Chemosphere 307, 135984. https://doi.org/https://doi.org/10.1016/j.chemosphere.2022.135984

The highlights of the manuscript '**The state-of-the-art development of biochar based photocatalyst for removal of persistent organic pollutants in wastewater'** are;

- Effective synthesis technique of photocatalyst using biochar as a substrate
- Changes in physico-chemical properties via different synthesis techniques
- Photocatalytic improvement due to the incorporation of biochar
- Effectiveness in treating different pollutants via photocatalysis

Declaration of interests

☐ The authors declare that they have no known competing financial interests or personal relationships that could have appeared to influence the work reported in this paper.

☒ The authors declare the following financial interests/personal relationships which may be considered as potential competing interests:

Mahesan Naidu Subramaniam reports financial support was provided by European Union. Zhentao Wu reports financial support was provided by European Union. Shouyong Zhou reports financial support was provided by The Royal Society.